

Computational flow analysis of cryogenic turboexpander

Salil Mohanty



Department of Mechanical Engineering
National Institute of Technology Rourkela

Computational flow analysis of cryogenic turboexpander

Thesis submitted in partial fulfillment

of the requirements of the degree of

Master of Technology

in

Mechanical Engineering

(Cryogenic and Vacuum Technology)

by

Salil Mohanty

(Roll Number: 214ME5437)

based on research carried out

under the supervision of

Prof. Ranjit K. Sahoo



May, 2016

Department of Mechanical Engineering
National Institute of Technology Rourkela

Dedicated to
My Family
&
The Almighty God



Department of Mechanical Engineering
National Institute of Technology Rourkela
Rourkela-769 008 , Odisha , India. www.nitrkl.ac.in

Prof. R.K.Sahoo
Professor

May , 2016

Certificate

This is to certify that the work carried out by *Salil Mohanty* in the thesis entitled *Computational flow analysis of cryogenic turboexpander* bearing Roll Number 214ME5437, is submitted to National Institute of Technology, Rourkela under my supervision and guidance for the award of the degree of *Master of Technology* in *Cryogenics and Vacuum Technology, Department of Mechanical Engineering*. To best of our knowledge the work carried out in this thesis is not submitted for any degree or academic award elsewhere.

R.K. Sahoo

Acknowledgement

It is my genuine pleasure to express my deep sense of thanks and gratitude to my mentor and guide *Prof. R.K. Sahoo Dept. of Mechanical Engineering, NIT, Rourkela*. His dedication, interest and helping attitude towards his student had been responsible for the completion of my research work. His knowledge, timely advice and scientific approach have helped me a lot in completion of my task.

I would specially thank to the Head of the Department, Mechanical engineering *Prof. S.S. Mahapatra* and all the faculty members of the Department of Mechanical Engineering, for providing me deep knowledge about various courses they had taught and also for providing me necessary technical suggestions during my research pursuit.

I thank profusely all my friends and the staff of Mechanical Engineering Department for their kind cooperation and timely help which allowed me to complete my research work in time and bring out this thesis.

I am privileged to thank my family for their encouragement throughout my entire journey, without which I would have struggled to find the inspiration and motivation needed to complete this thesis.

Salil Mohanty

Roll no. 214ME5437

Cryogenics and vacuum technology

Abstract

In many kind of cryogenic process plant (e.g. - nitrogen and helium liquefier, air separation units) expansion turbine is the most critical part. A cryogenic process plant consists of many components such as compressor, expansion turbine, heat exchanger, chilling and purification units. In the expansion turbine the temperature of the gas decreases due to the reduction in the pressure and helps in producing the lowest temperature in the refrigeration plant. A cryogenic turboexpander is a highly precise device as it is used at very high speed with a bearing clearance of 10 to 40 μm and the rotor is balanced properly. Special attention is given towards the selection of material, tolerance, fabrication and assembly of the cryogenic turboexpander.

This project basically deals with the design and fluid flow analysis of the expansion turbine. The determination of the turbine profile is done by taking data from the design charts which are based on the similarity principles. The method given by the Hasselgruber is used for determining the turbine blade profile. The software packages used for fluid flow simulations are ANSYS bladegen, turbogrid and CFX. The blade is modelled in bladegen by taking the hub and shroud data of the blade profile. For meshing of the turbine model turbogrid is used. For fluid flow simulation purpose CFX-pre is used to specify the parameters at inlet and outlet of the turbine and CFX-post is used for determining and analysing the results.

Variation in temperature, entropy, velocity and mach number is determined along the streamline through different graph plots.

Contents

Certificate

Acknowledgement

Abstract

List of tables

List of figures

Nomenclature

| | |
|---|-----------|
| Chapter 1: Introduction | 1 |
| 1.1 About turboexpander..... | 2 |
| 1.2 Anatomy of cryogenic turboexpander..... | 3 |
| 1.3 Aim of present investigation..... | 4 |
| 1.4 Organization of the thesis..... | 5 |
| Chapter 2: Literature Review | 7 |
| 2.1 Historical development of turboexpander..... | 8 |
| 2.2 Design of turboexpander..... | 11 |
| Chapter 3: Theory | 16 |
| 3.1 Design of Turboexpander..... | 17 |
| 3.1.1 Fluid parameters and layout of component..... | 17 |
| 3.1.2 Design of turbine wheel..... | 19 |

| | |
|---|-----------|
| 3.1.3 Blade profile determination..... | 21 |
| Chapter 4: Computational fluid flow analysis | 24 |
| 4.1 Design of expansion turbine in bladen..... | 25 |
| 4.2 Meshing of the turbine model..... | 28 |
| 4.3 Physic definition of meshed model in CFX-Pre..... | 31 |
| 4.4 Solution of flow by means of CFX solver..... | 33 |
| 4.5 Obtaining result in CFX-Post..... | 35 |
| Chapter 5: Result and discussion | 36 |
| 5.1 Streamwise variation of pressure from inlet to outlet..... | 36 |
| 5.2 Streamwise variation of temperature from inlet to outlet..... | 37 |
| 5.3 Streamwise variation of velocity from inlet to outlet..... | 39 |
| 5.4 Streamwise variation of Mach number | 39 |
| 5.5 Streamwise variation of density from inlet to outlet..... | 40 |
| 5.6 Streamwise variation of entropy..... | 42 |
| 5.7 Streamline variation at trailing edge of the blade..... | 43 |
| Chapter 6: Conclusion and future work | 46 |
| 6.1 Conclusion..... | 47 |
| 6.2 Future work..... | 47 |
| References | 48 |

List of tables

| | |
|--|----|
| Table 3.1: Basic input parameter for expansion turbine of turboexpander..... | 17 |
| Table 3.2: Thermodynamic state at turbine outlet..... | 20 |
| Table 3.3: Thermodynamic state at turbine inlet..... | 21 |
| Table 3.4: Coordinates for Blade Profile generation..... | 22 |
| Table 3.5: Turbine blade profile co-ordinates | 23 |
| Table 4.1: Physics definition for turbine rotor | 32 |
| Table 5.1: variation of thermodynamic properties..... | 36 |

List of figures

| | |
|--|----|
| Figure 1.1: cryogenic refrigeration cycle with and without expansion device..... | 3 |
| Figure 1.2: schematic view of cryogenic turboexpander..... | 4 |
| Figure 2.1: ns-ds diagram for radial inflow turbines..... | 13 |
| Figure 3.1: Longitudinal section of turboexpander displaying various components..... | 18 |
| Figure 4.1: Meridional blade profile..... | 26 |
| Figure 4.2: Variation of Beta and Theta at different spans..... | 26 |
| Figure 4.3: Variation of Beta and Theta..... | 27 |
| Figure 4.4: Wireframe model of turbine generated in bladegen..... | 27 |
| Figure 4.5: Solid model of turbine in bladegen..... | 28 |
| Figure 4.6: view of turbine rotor after bladegen import..... | 29 |
| Figure 4.7: view of the turbine rotor after mesh topology is set..... | 30 |
| Figure 4.8: view of the turbine rotor after meshing..... | 31 |
| Figure 4.9: direction of flow at inlet and outlet..... | 33 |
| Figure 4.10: Wireframe and Meridional model of turbine rotor..... | 35 |
| Figure 5.1: variation of pressure from inlet to outlet..... | 38 |
| Figure5.2: Isometric view of pressure variation..... | 39 |
| Figure 5.3: Temperature variation along streamwise inlet to outlet..... | 40 |
| Figure 5.4: Isometric 3D view of temperature variation..... | 40 |
| Figure 5.5: Variation of velocity from inlet to outlet..... | 41 |
| Figure 5.6: Streamwise variation of Mach number..... | 42 |

| | |
|---|----|
| Figure 5.7: Variation of density from inlet to outlet..... | 43 |
| Figure 5.8: Streamwise variation of Entropy..... | 44 |
| Figure 5.9: Streamline variation at trailing edge of the blade..... | 45 |

Nomenclature

| | | |
|----------------|----------------------|---------------------------------------|
| D | diameter (wheel) | (m) |
| d | diameter (shaft) | (m) |
| E | entropy | (J kg ⁻¹ K ⁻¹) |
| h | enthalpy | (J/kg) |
| K _e | free parameters | (dimensionless) |
| K _h | free parameters | (dimensionless) |
| M | mach number | (dimensionless) |
| N | rotational speed | (rev/min) |
| n _s | specific speed | (dimensionless) |
| P | pressure | (N/m ²) |
| Q | volumetric flow rate | (m ³ /s) |
| r | radius | (m) |
| S _E | energy source | (kg m ⁻¹ s ⁻³) |
| S _M | momentum source | (kg m ⁻² s ⁻²) |
| T | temperature | (K) |
| t | blade thickness | (m) |
| U | velocity magnitude | (m/s) |
| Z | number of vanes | (dimensionless) |

Greek symbols

| | | |
|----------|-----------------------|---------------------------------------|
| ρ | density | (kg/m ³) |
| τ | shear stress | (kg m ⁻¹ s ⁻²) |
| ω | rotational speed | (rad/s) |
| θ | tangential coordinate | (dimensionless) |

Subscripts

| | |
|----|-----------------------------|
| 0 | stagnation condition |
| in | inlet to the nozzles |
| 1 | exit from the nozzles |
| 2 | inlet to the turbine wheel |
| 3 | exit from the turbine wheel |

Chapter 1

INTRODUCTION

Introduction

1.1 About Turboexpander

Turboexpander is often defined as a radial expansion turbine and a centrifugal compressor coupled together as one unit. The expansion turbine is the heart of modern cryogenic turboexpander. Power is produced from a highly pressurized process gas which flows inside the expansion turbine and causing the shaft rotation by using the kinetic energy of the gas. The brake compressor extracts work output from the expansion turbine. The vertical mounting of the shaft reduces the radial load on bearing. The alignment of the shaft is maintained by absorbing the axial and radial load which is done by placing each pair of radial journal and axial thrust bearing.

Though there is an abundance of gaseous materials in our atmosphere (nitrogen, oxygen, argon) and below crust of the earth (fossil fuel, helium) we require to use and keep them for significant purposes. In today's world the amount of consumption of the above mentioned materials is the parameter for measuring the technological growth of a society. The liquefaction of gas is required for large scale storing, transporting, and for low temperature uses. Atmosphere is the only source of gases like nitrogen, argon and oxygen, so for large scale production of these gases low temperature liquefaction is the best economical way. Other industrial applications are production of super conducting magnets, cutting tool treatment, SQUID magnetometers, preserving blood cell, which requires cryogenic temperature. There are several ways in which common gas can be liquefied for which there is low temperature requirement. In the early years of 20th century linde and heylandt cycles were commonly used which are high pressure cycles to liquefy helium and hydrogen, but in recent years low pressure cycle based cryogenic process plant are almost used everywhere. Turbine based plant have higher thermodynamic efficiency in comparison with high and intermediate pressure devices. Turbine based plant are also highly reliable and can be easily integrated with other devices. For some time reciprocating expanders were used but due to increase in efficiency and reliability of expansion turbines, use of reciprocating expanders are almost eliminated.

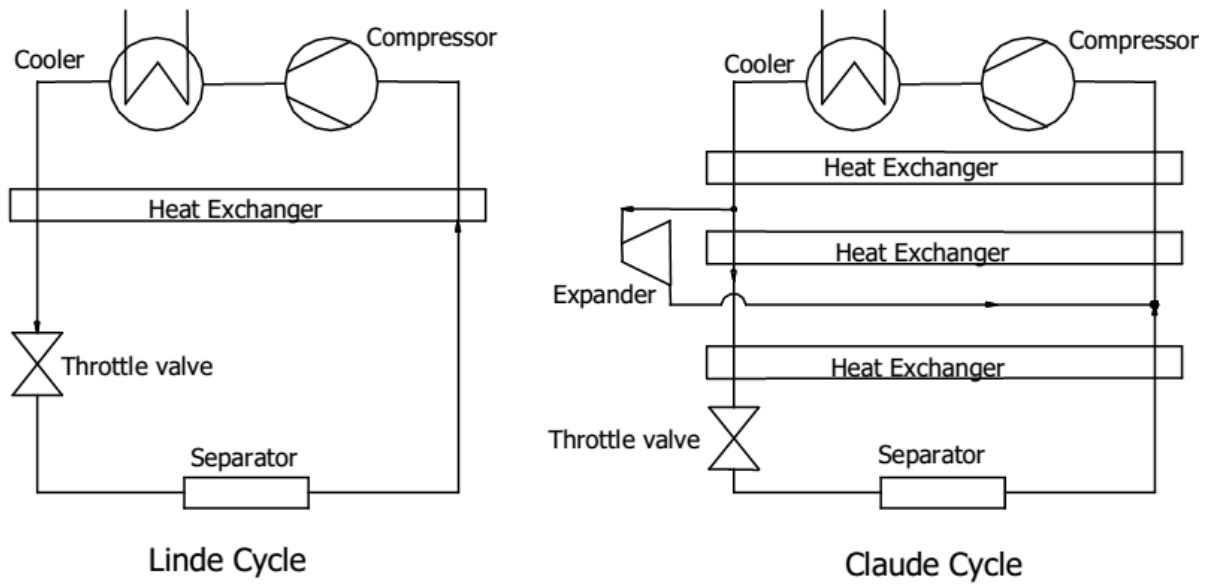


Fig 1.1 cryogenic refrigeration cycle with and without expansion device

Various uses of expansion turbine are:

1. Providing air condition in aeroplane by generating refrigeration.
2. Separation of hydrocarbon and propane from natural gases in petroleum industries.
3. Used in extraction of energy e.g. refrigeration
4. Recovery of power from wellhead natural gas which is at high pressure.
5. Waste energy recovery in paper industries

1.2 Anatomy of cryogenic turboexpander

The essential component of a cryogenic turboexpander are expansion turbine, brake compressor which are attached on a shaft and backed by a number of thrust and journal bearing. Appropriate housing is provided to hold these components in place with fluid inlet and exit ducts.

Following are the basic parts of turboexpander:

1. Cold end housing: highly pressurized gas enter through this.
2. Nozzle: Fluid gets accelerated through this at the expense of kinetic energy.
3. Expansion turbine: The accelerated fluid from the nozzle is impinged upon the blades of the turbine

4. Diffuser: A diverging section which is used to convert kinetic energy of the fluid to pressure energy.
5. Loading device: It is generally a compressor which is used for extraction of work output.
6. Shaft: It is used for connecting the expansion turbine with the brake compressor.
7. Journal bearing: It is used for balancing the load and alignment of the rotor.
8. Thrust bearing: The difference in pressure created in between the brake compressor and expansion turbine is supported by the thrust bearing.
9. Bearing housing: It houses the bearing at proper place.
10. Seals: The fluid leakage is prevented by providing the seals.

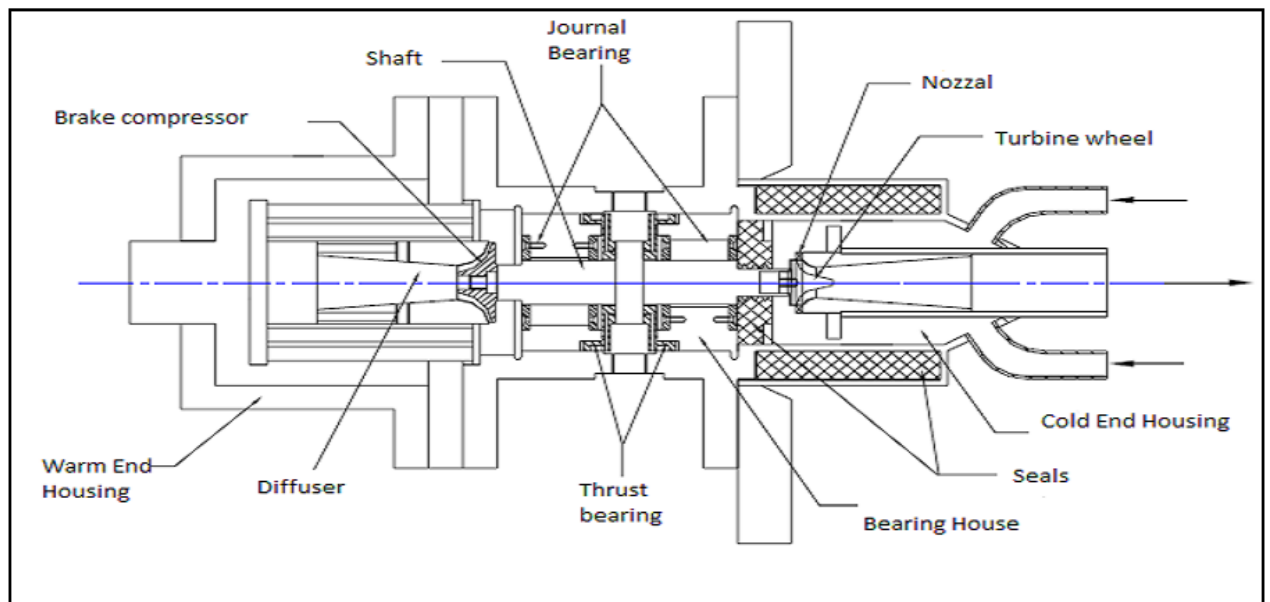


Fig. 1.2 schematic view of cryogenic turboexpander

1.3 Aim of present investigation:

In recent years there is a shift in technology in developed countries where high and medium pressure cycles has been replaced by low pressure turbine based cycles. Therefore now a days turboexpander has become a very important part of any cryogenic refrigeration plants. Industrially developed countries have bought perfection in this technology and it is being produced commercially, but this technology has remained mostly proprietary so there is a need of developing this technology indigenously for our country.

For the development of the expansion turbine of the turboexpander this project has been undertaken. The objectives are:

- i. Determining the blade geometry of the expansion turbine using the method given by Hasselgruber.
- ii. By using the determined geometry, construct a computational model of the turbine.
- iii. Study the fluid flow performances of the turbine.

For computational flow analysis following specification are taken for the turboexpander:

| | |
|---------------------------------|--------------|
| Working fluid | : nitrogen |
| Temperature at inlet of turbine | : 99.65 K |
| Pressure at inlet of turbine | : 3 bar |
| Pressure at outlet of turbine | : 1.28 bar |
| Mass flow rate | : 0.024 Kg/s |

1.4 Organization of thesis

This thesis is parted into six chapters. Chapter-I gives a concise introduction to cryogenic expansion turbine and its application in various process. The need of the development and the objective of the investigation is provided. Chapter-II gives a wide survey of various literature available on cryogenic expansion turbine. With a vivid historical development this chapter gives a wide outline of many technical issues connected to development of expansion turbine.

Chapter–III articulates an organized design method based upon published works which are designed and authenticated for the development of expansion turbine. In this chapter a detailed description of fluid parameters, component layout, design of expansion turbine and blade profile determination is given from previous research works.

Chapter-IV elaborates the computational set up for studying the performance of turbine. This chapter describes the designing of turbine model in bladegen, meshing of model in turbogrid and about CFX simulation

The results obtained after the CFX simulation is shown in chapter-V. A number of graphs and contour are plotted in this chapter. Conclusion of the thesis and the scope for future work is provided in chapter-VI.

Chapter 2

Literature review

Literature review

As already mentioned expansion turbine is one of the most vital part of a cryogenic turboexpander. Turboexpander in any cryogenic device acts as the primary cold generating device so its characteristic such as efficiency and reliability to a great level impacts the cost parameter of the cryogenic process plant.

Due to the broad practical uses of the turboexpander it has drawn the attention of great number of researcher over many years. Investigation contributing both applied and fundamental research and studies contributing experimental and theoretical have been accounted in literature.

Basic operating conditions, design as well as construction processes have been well documented in textbooks on cryogenic technology and turbomachinery [1-14]. The textbooks [1, 3, 4] gives a splendid introduction to the domain of cryogenic technology and consists of valuable information on the turboexpander. The textbook provided by Devydov [5] consist vivid description of the basic principles of computation and design method of dimensionally small and high velocity cryogenic turboexpander. The textbook given by Bloach and Soars [6] latest overview of the turboexpander and the places where these machineries are applied in an advanced cost witting process plant surroundings. The elaborated loss computation and process of analysing the performance are briefed by Whitfield and Baines [13, 14].

Journals in the field of cryogenics and turbomachines and important conferences on advanced cryogenic engineering and at international cryogenic engineering conference dedicate an ample amount of their research towards the development of turboexpander.

2.1 Historical development of turboexpander

Lord Rayleigh provided the concept of using the expansion turbine for liquefying gases by introducing in the cycle. He was the first to introduce this concept through a letter to “nature” on 28th June, 1898 [15]. He proposed replacing of the piston expander with expansion turbine to liquefy the air. Rayleigh stressed on the matter that the most significant purpose turbine

would be refrigeration aspects instead of power recovery. In the year 1898, an engineer from Britain named Edgar C. Thrupp made a simple air liquefying machine using a turbine which was patented by him [16]. This expander was a kind of double flow equipment in which cold air enters at the centre and gets divided into two streams which flow in opposite direction. During the same period an American named Joseph E. Johnson patented a device for gas liquefying purposes. A single stage (De Laval) impulse turbine expander was used by him. Other patents in the early 20th century include the expansion turbine provided by Davis (1922). The first commercially successful practical application of a cryogenic expansion turbine was published in the year 1934 by a German company named Linde Works [15]. They used an axial flow, single stage machine liquefying and separating air in a low pressure cycle, but within two years it was substituted with an impulse turbine having inward radial flow.

In 1939 Kapitza published a brief description of a low temperature expansion turbine. In this he elaborated about a turbine that attained 83% efficiency. The turbine wheel was of 8 cm monel and consisting of straight blades and worked at 40,000 rpm [17]. In 1942 The National Defence Research Committee of USA sponsored a programme that developed a turboexpander which worked without any glitch for periods combining 2,500 hrs and attained an efficiency greater than 80% [17]. An impulse type expansion turbine was used by the German throughout the 2nd world war for their oxygen gas systems [18].

In the mid-fifties Sixsmith commenced a work on turboexpander based on small gas bearing on a machine at Reading University for a minor air liquefying plant [19]. The Atomic Energy Authority of the United Kingdom in 1958 built up an inward flow radial turbine for a nitrogen producing plant [20]. In between 1958 and 1961 Stratos Division of Fairchild Aircraft Co. developed a turboexpander with blower as the loading device, largely for air separating units [18]. A high speed expansion turbine was designed by Voth et. al for Argonne National Laboratory as a contribution towards a cold moderate refrigerator [21]. For the first time in 1964 a commercially expansion turbine was operated using helium for the bubble chamber of Rutherford helium plant. It produced 73W at 3K [19].

General Electric Company, New York in 1968 developed a high speed turbo alternator using a gas bearing system, which ran at low loss and was capable of producing cryogenic temperature [22-23]. National Bureau of Standards at Boulder, Colorado [24] designed a turbine which was 8mm in diameter operating at 30 K inlet temperature and 600,000 rpm

speed. Sulzer Brothers of Switzerland designed a turboexpander in 1974 for cryogenic systems with automatic gas bearings [25]. Cryostar of Switzerland developed a cryogenic turboexpander in 1981 by integrating active magnetic bearing radially and axially [26]. There was a wide experimental testing in 1984 done on a medium sized prototype turboexpander for liquefying nitrogen. At Hitachi, Ltd., Japan Izumi et. al [27] designed a mini turboexpander for a helium refrigeration system which worked on claudé cycle. It consisted of a reaction turbine with radial inward flow. The wheel diameter of the turbine was 6mm and diameter of the shaft was 4mm. The first and second stage turboexpander has a rotational speed of 816,000 and 519,000 rpm respectively.

Kun et. al [28–30] suggested a very simple method for the development of a highly efficient expansion turbine. In 1979 Kun & Sentz [29] started surveying the operating plants for rendering the cost factor related to turbine. With the collaboration of Goddard Space Flight Centre of NASA Sixsmith et. al. [31] designed a mini turbine for cryocoolers worked on brayton cycle. The turbine was of 1.5mm in diameter rotating approximately at a speed of 1,000,000 rpm.

A two stage mini turbine was developed by Yang et. al [33] for a helium liquefier having capacity 1.5 L/hr at the Cryogenic Engineering Lab of the Chinese Academy of Science. The rotational speed of the turbine was greater than 500,000 rpm. National Bureau of Standards USA developed a small expansion turbine which operated at the speed of 600,000 rpm in a gas bearing which was externally pressurized [34].

Naka Fusion Research Centre having affiliation to Japan Atomic Energy Institute developed a wet type turboexpander for helium refrigeration with 70% adiabatic efficiency [36-37]. The turboexpander was having a shaft diameter of 40mm, impeller diameter of 59mm and automatic thrust and gas journal bearing [36]. A radial turbine with high expansion ratio was developed by Ino et. al [38–39] for liquefying helium which has a capacity of 100L/hr. It was operated with 70 MW superconductive generators.

Davydenkov et. al [40] in Moscow, Russia designed a turboexpander having a foil bearing for helium liquefying systems. The utmost rotational speed of the turbine was 240,000 rpm having shaft diameter 16mm. The third stage of the turboexpander was developed in 1991,

by “Cryogenmash” [41] for the gas expansion system. “Heliummash” [41] designed similar turboexpander for each stage, varying only in dimensions.

The incorporation of foil bearing which are hydrodynamic gas lubricated with TC-3000 expansion turbine was done by ACD Company [42]. In the reference [43] elaborately specifies the modules of the turboexpander constructed by the company.

In the particle accelerator centre of Fermi National laboratory, USA Sixsmith et. al. [47] designed a mini wet expansion turbine for helium liquefying purpose. The shaft of the turboexpander was supported by the highly pressurised gas bearing and was having a turbine rotor of 4.6mm at cold end and a brake compressor of 12.7mm at warm end. The expander operated at a speed of 384,000 rpm and 444 watts of cooling capacity. At the institute of cryogenic engineering, China Xiong et. al. [48] designed a turboexpander having 103mm long rotor and of 0.9N weight, which worked at a speed of 230,000 rpm. Experiment was conducted on the turboexpander by using two types of gas lubricated foil journal bearings. For more than 30 years L’Air liquid company, France has produced more than 350 units operating all over the world both industrially and research purposes [49,50]. These turbines uses hydrostatic gas bearing, which provides unique versatility with calculated mean failure time of 45,000 hours. Active magnetic bearings was used as the substitute to oil bearing system by Atlas Copco [51].

India has been dawdling behind many countries in this area of research and development. Still remarkable advancement has been done during last two decades. Jadeja et. al [52–54] at CMERI Durgapur designed a inward radial flow turbine which uses gas bearing as support for cryogenic process plants. This device operated at around 40,000 rpm. This programme was quitted before any substantial advancement could be accomplished. At IIT Kharagpur a turboexpander was designed using an aerostatic thrust and journal bearings which operated at 80,000 rpm. The detailed technical features is given in the PhD thesis of Ghosh [55].

2.2 Design of turboexpander

The procedure for designing turboexpander is not straightforward. The manufacturing of turboexpander is the outcome of various engineering subjects: fluid mechanics, machine dynamics, vibration analogy, tribology, stress analysis, controls and fabrication. Parameters

such as flow rate, inlet pressure, outlet pressure, inlet temperature and gas composition [56]. The basic constituents of a turboexpander, its design procedure and development is intended to be discussed in this section.

Turbine wheel

In the past twenty years, performance chart has been widely used for the representation of the characteristics of turbomachinery [57]. There are many characteristic value that are used for determination of major performance standards of turbomachines, for example velocity ratio of turbine (U/C_o), flow coefficient factor, specific speed and pressure ratio [58]. An easier method has been provided by Balje for the calculation of efficiency of the radial turbines and for finding out their characteristic [59]. Similarity principles gives a favourable and practical method to know the significant characteristic of the turbomachines. According to Similarity principles two parameters are enough to decide the major dimensions and the velocity triangles at inlet and exit of the turbine wheel. The specific speed and specific diameter altogether determine the dynamic similarity. The physical significance of the two parameter n_s , d_s is that, fixed values of specific diameter d_s and specific speed n_s combined permits the similar flow condition exist in geometrically similar turbo machineries.

Specific speed and specific diameter

The general idea of specific speed was first brought in for classification of hydraulic machines. This parameters was introduced by Balje [58] for the development of gas turbines and compressors. For getting the maximum possible value of polytropic efficiency and to construct an optimum geometry corresponding value of specific diameter and specific speed are selected [56]. Specific speed is a very useful parameter for the designing of the compressible flow rotodynamic machine [60]. The design chart provided by balje [8, 58, 61] is very widely used on various turbomachines. These diagram helps in the calculation of maximum achievable efficiency and the most favourable design geometry with related to specific speed and specific diameter for a fixed Reynolds and laval number [8]. A n_s - d_s diagram for mixed flow type radial inflow turbine with blade angle 90° is provided in figure 2.1.

A major benefit of Balje's chart is that the efficiency is expressed as the function of the parameters which are of most concern to the designer, namely rotor diameter and angular speed. The n_s - d_s diagram provided by Balje [8] has been found out for specific heat ratio $\gamma = 1.41$. If the working fluid is changed the value of γ will change (e.g. helium has $\gamma = 1.67$), so the chart needs to be modified. It has been shown by Macchi [62] that for small pressure ratio this effect is minimum but for higher values it becomes important.

Rohlik [63] stated that, for radial flow turbine to get an optimum value of static efficiency and total efficiency, the value of specific speed is taken as 0.58 and 0.93. A plot between total and static efficiency has been plotted for the specific speed between 0.46 and 0.63. According to Luybli and Filippi [64] significant losses in nozzles, regions of rotating disc and vaneless zones are observed in the turbines having less specific speed while turbines with higher specific speed have more exit velocity losses. The specific diameter and specific speed are also known as shape parameters [12] and also sometimes cited as design parameter, because the shape decides which design to be chosen. For maximum efficiency [30] a cryogenic turboexpander is designed at a specific speed of 0.5 and specific diameter of 3.75. Kun and Sentz [29] took the value of n_s as 0.54 and the value of d_s as 3.72. Swift [34] designed a mini turbine for helium refrigeration having two stage expansion with the value of n_s as 0.09 and 0.14.

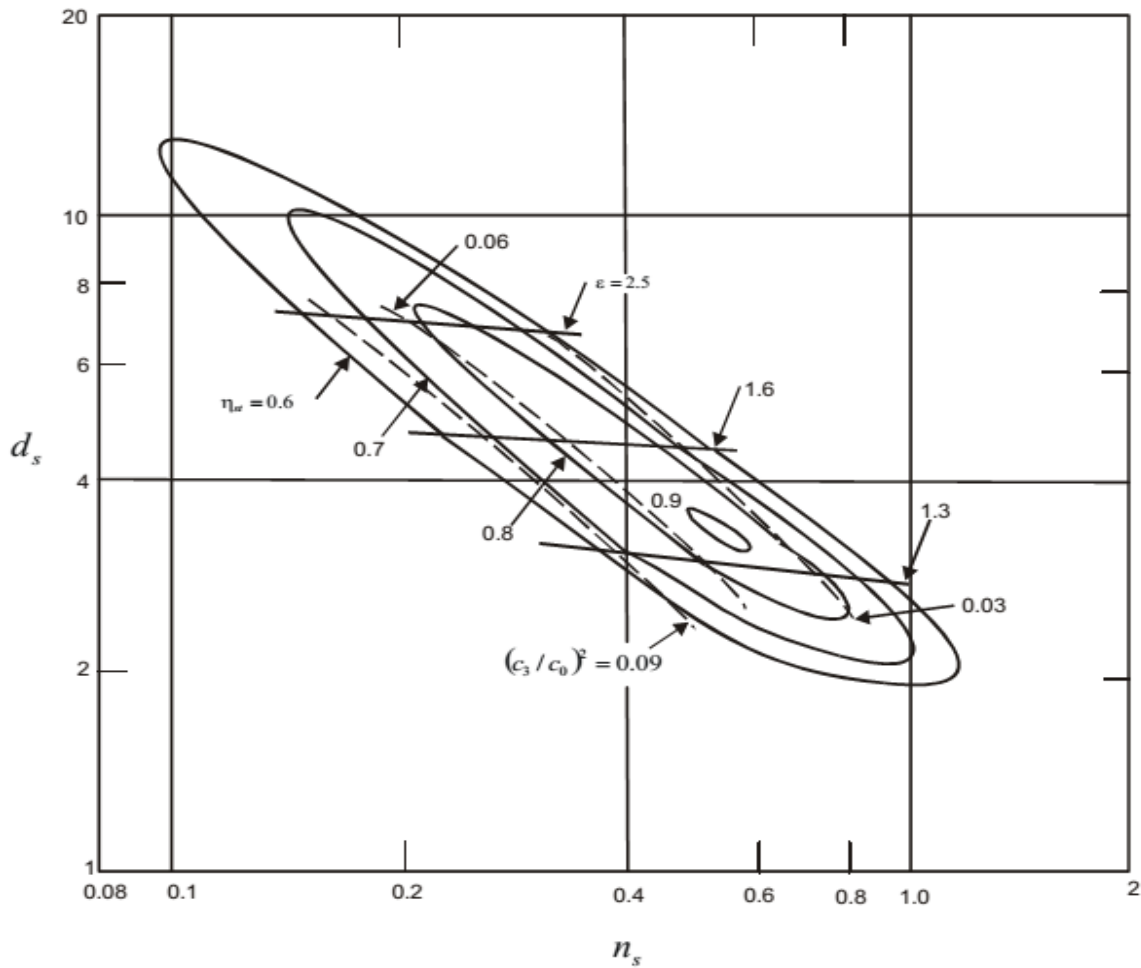


Fig 2.1: n_s - d_s diagram for radial inflow turbines with $\beta_2 = 90^\circ$ (from Ref. [8], Fig. 5.110)

One major trouble in using the specific speed norms in gas turbine comes due to the compressibility nature of the fluid [65]. Vavra has shown that specific speeds doesn't depend upon the velocity ratio (U/c_0) and the turbine dimensions, therefore they don't depend upon the Mach number and the Reynolds number. As a consequence specific speed do not satisfies the dynamic similarity principles if the compressibility factor of the working fluid is taken into consideration. Attempts to associate the losses solely to specific speed, by applying it as the only criteria for assessing a design are not only wrong at fundamental level but also it creates a false notion about the modern development, thereby creating hindrance in research work that gives a healthy design criteria.

Parameters

The ratio between the exit tip diameter and inlet diameter is confined to utmost value of 0.7, this prevents excess shroud curvature. In the same way the excess of blockage in hub blade and losses are prevented by keeping the exit hub diameter to tip diameter ratio to a minimal value of 0.4 [63,60]. Kun and Sentz [29] have assumed $\epsilon = 0.68$. The ratio between the exit diameter at meridian to rotor inlet diameter is taken as 0.625 by Balje [59]. The blade height to blade diameter at inlet should lie between 0.02 and to 0.6 [60].

At inlet of the turbine, peripheral component of absolute velocity varies with the nozzle angle. This component of velocity varies with blade angle at exit and peripheral speed at outlet [59]. Balje [59] has shown that the suitable ratio of meridional element of inlet absolute velocity and absolute velocity at exit of the turbine wheel is related to the mach number and flow factor. Balje took the value of ratio between inlet and exit meridional element of absolute velocity for a radial flow turbine as 1. The general perception is that the maximum incidence angle varies with the no. of blade and it lies in between -20° and -30° . The mach number at inlet is minimized by selecting the absolute flow angle or it can also be deduced from the velocity ratio (U/C_o), as 0.7. The absolute flow angle is generally selected in between 70° and 80° .

Number of blades

A simple blade load distribution has been assumed by Balje [8] to derive an equation for minimum number of the rotor blade which varies with the specific speed. A guide for choosing the number of blade has been provided by Denton [67]. This theory ensures that at the pressure surface there is no flow stagnation. He suggested that the 12 number of blade are optimum for cryogenic turbines. To reduce excess frictional losses and the variation of flow between neighbouring blades, the optimum number of blade has been provided by Wallace [68].

Rohlik [63] proposed a procedure to compute number of blade by considering the flow separation factor in the turbine passage. In this procedure the number of blades are chosen so that to control the boundary layer formation in the flow passage.

Chapter 3

Theory

THEORY

3.1 Design of turboexpander

This chapter gives the detailed experimental design procedure for the turboexpander and the analysis of related cryogenic processes. These complete unit consist of expansion turbine, brake compressor, shaft, nozzle, diffuser, thrust and journal bearing with proper housing. The design method of cryogenic turboexpander relies upon working fluid, inlet conditions, expansion ratio and flow rate. The method provided in the current chapter grants any arbitrary combination of fluid species, expansion ratio and inlet conditions because the properties of fluid is thoroughly taken into consideration in the related equations. The computing process has been exemplified with examples. The current design process is more organised and transparent than any open literature [55]. The design process of cryogenic turboexpander comprises following unit, which are briefed in the following sections.

- Fluid parameter and layout of component
- turbine wheel Design
- Blade profile determination

3.1.1 Fluid parameter and layout of component

The specifications of the fluid have been provided by the demands of small refrigerator producing much less than 1 Kw refrigeration. By the workers experience, a turbine of 75% efficiency has been presumed [20, 33, 67, 69]. The temperature at the inlet has been assigned rather randomly, chosen in a way that exit state doesn't come under the two phase area even when it is ideal or isentropic expansion. The fundamental input parameters are provided in table 3.1.

| | |
|------------------------------|------------|
| Working fluid | Nitrogen |
| Temperature at turbine inlet | 122K |
| Pressure at turbine inlet | 6.0 bar |
| Pressure at turbine outlet | 1.5 bar |
| Mass flow rate | 0.023 kg/s |
| Anticipated efficiency | 75% |

Table 3.1 Fundamental input parameter for expansion turbine of turboexpander

An assembly of turboexpander constitute the following fundamental units:

- The expansion turbine, diffuser and nozzle
- Shaft
- Brake compressor
- Pair of thrust and journal bearing
- Proper housing

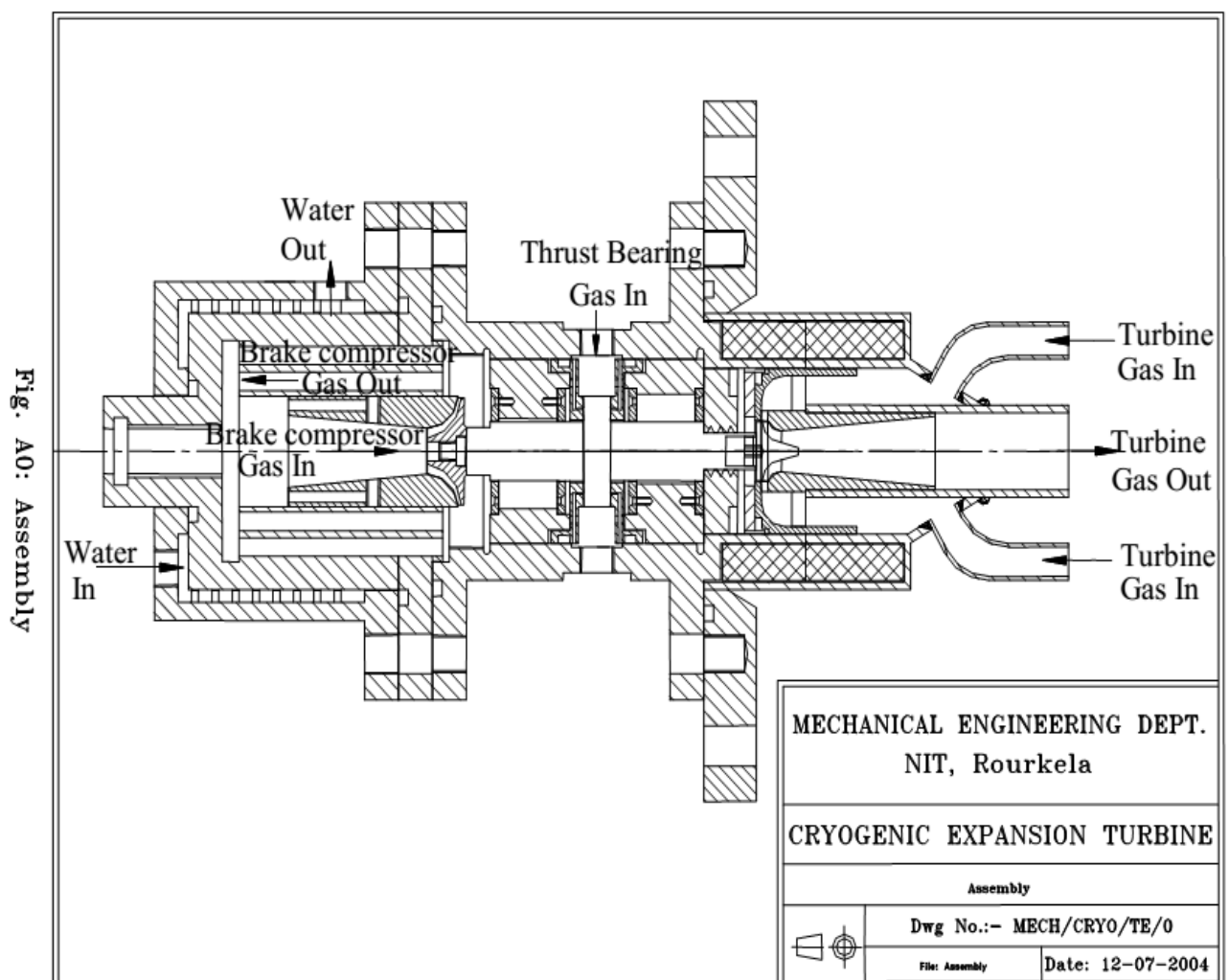


Figure 3.1 Longitudinal section of turboexpander displaying various components

The longitudinal view of a cryogenic turboexpander is shown in Fig. 3.1, displaying different component of the system. The finished system has three significant component – rotor,

bearing and housing. In addition to this there are also many other critical component such as fasteners, spacers and seals.

3.1.2 Design of turbine wheel

The turbine wheel design is done by the procedure described by Balje [8] and Kun and sentz [29] that are established upon the “similarity principles”. The law of similarity states that if Reynolds number, specific heat ratio and Mach number of working fluid are provided, to achieve the best geometry for optimum efficiency two dimensionless parameter: specific speed and specific diameter unambiguously determine the significant dimensions of the wheel and the velocity triangles at inlet and exit. Specific speed and specific diameter is characterized as:

$$\text{Specific speed } N_s = \frac{\omega \times \sqrt{Q_3}}{(\Delta h_{in-3s})^{3/4}}$$

$$\text{Specific diameter } D_s = \frac{D_2 \times (\Delta h_{in-3s})^{1/4}}{\sqrt{Q_3}}$$

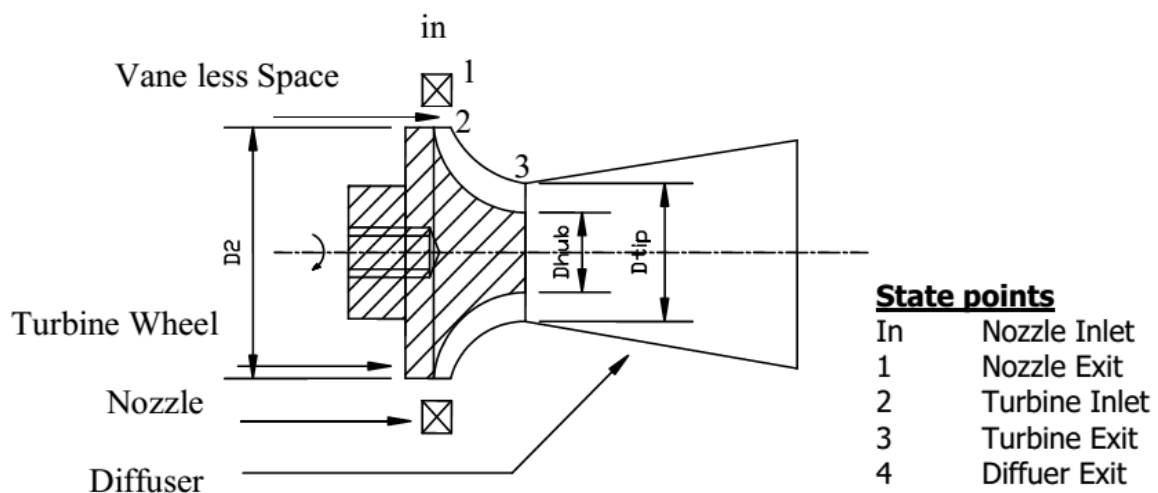


Figure 3.2: Turboexpander state points

In the equation of n_s and d_s , Q_3 is the volumetric flow rate at the exit of turbine wheel. The real values of h_{3s} and Q_3 , which helps in defining n_s and d_s are unknown priori. However Kun and Sentz [29] suggested a pair of empirical factor K_1 and K_2 for the calculation of these parameters.

$$Q_3 = K_1 Q_{ex}$$

$$\rho_3 = \rho_{ex} / K_1$$

$$\Delta h_{in-3s} = K_2 (h_{0in} - h_{exs})$$

K_1 and K_2 gives the difference between the states at '3' and 'ex' which is caused by the pressure recovering and resultant increase in density and temperature.

The important dimensions of the prototype turbine has been calculated by S.K. Ghosh [52], they are as follows:

Rotational speed: $N = 218790 \text{ rpm}$

Diameter of the wheel: $D_2 = 16.0 \text{ mm}$

Diameter of eye tip: $D_{tip} = 10.8 \text{ mm}$

Diameter of eye hub: $D_{hub} = 4.6 \text{ mm}$

Numbers of blades: $Z_{tr} = 10$

Blade thickness: $t_{tr} = 0.6 \text{ mm}$

The value of Thermodynamic properties at the outlet of the turbine has been calculated by S.K. Ghosh [52]. These values at wheel discharge (state 3) has been provided in table 3.2.

| | Stagnation value | Static value |
|------------------------------|------------------|--------------|
| Pressure (bar) | 1.505 | 1.29 |
| Entropy (kJ/kg.K) | 5.452 | 5.452 |
| Temperature (K) | 90.02 | 85.96 |
| Density (kg/m ³) | 5.89 | 5.26 |

3.2 Thermodynamic state at turbine outlet

The values of thermodynamic property at wheel inlet

| | Stagnation value | Static value |
|------------------------------|------------------|--------------|
| Pressure (bar) | 2.872 | 2.453 |
| Entropy (kJ/kg.K) | 5.335 | 5.335 |
| Temperature (K) | 99.65 | 90.45 |
| Density (kg/m ³) | 10.312 | 9.728 |

Table 3.3 Thermodynamic state at turbine inlet

3.1.3 Blade profile determination

To maximise the performance of the turbine a computational process is defined to design the blade profile. The computation of three dimensional blade profile contour and at the same time the velocity, temperature and pressure profiles of the turbine wheel has been described in an elaborated procedure. Hasselgruber [86] has suggested the procedure for computing the blade profile and the work has been led by Kun & Sentz [29]. The length and curvature of flow path affects the loss in fluid pressure, while fluid passing through the turbine blade. Therefore two parameters has been determined by Hasselgruber [86] i.e. K_e and K_h to check the flow path and its curvature. The magnitude and direction of the velocity helps in determining the most efficient blade profile for the turbine. It has been found out that the value of K_e remains in between 0.75 and 1 and for k_h the value varies between 1 and 20.

For the selection of the most suitable value of K_e and K_h the points has to be taken into consideration.

- The optimum value of efficiency
- The operating condition must be steady and uniform

- Manufacturing of blades should be easy

S. K. Ghosh [53] has found out the optimum value of parameters $K_e = 0.75$ and $K_h = 5.0$ which gives a better blade profile for the turboexpander.

The blade profile co-ordinate of mean surface, pressure surface and suction surface are shown in the table 3.4 and 3.5

| Tip Camber line | | | Hub Camber line | | |
|-----------------|-------|----------------|-----------------|-------|----------------|
| z(mm) | r(mm) | θ (deg) | z(mm) | r(mm) | θ (deg) |
| -0.24 | 5.38 | 0 | 0.24 | 2.32 | 0 |
| 0.24 | 5.29 | 6.71 | 0.67 | 2.56 | 6.71 |
| 0.71 | 5.22 | 12.39 | 1.11 | 2.76 | 12.39 |
| 1.18 | 5.19 | 17.19 | 1.55 | 2.94 | 17.19 |
| 1.63 | 5.18 | 21.22 | 2 | 3.1 | 21.22 |
| 2.08 | 5.19 | 24.58 | 2.46 | 3.25 | 24.58 |
| 2.52 | 5.22 | 27.37 | 2.93 | 3.4 | 27.37 |
| 2.95 | 5.27 | 29.65 | 3.39 | 3.56 | 29.65 |
| 3.37 | 5.33 | 31.49 | 3.86 | 3.72 | 31.49 |
| 3.79 | 5.41 | 32.96 | 4.33 | 3.91 | 32.96 |
| 4.19 | 5.51 | 34.1 | 4.79 | 4.13 | 34.1 |
| 4.58 | 5.63 | 34.96 | 5.24 | 4.37 | 34.96 |
| 4.97 | 5.78 | 35.61 | 5.68 | 4.65 | 35.61 |
| 5.34 | 5.95 | 36.06 | 6.09 | 4.97 | 36.06 |
| 5.69 | 6.16 | 36.38 | 6.47 | 5.32 | 36.38 |
| 6.02 | 6.4 | 36.58 | 6.81 | 5.7 | 36.58 |
| 6.33 | 6.68 | 36.7 | 7.11 | 6.11 | 36.7 |
| 6.62 | 6.99 | 36.77 | 7.37 | 6.54 | 36.77 |
| 6.87 | 7.33 | 36.8 | 7.59 | 6.99 | 36.8 |
| 7.09 | 7.7 | 36.81 | 7.76 | 7.45 | 36.81 |
| 7.28 | 8.1 | 36.81 | 7.9 | 7.92 | 36.81 |

Table 3.4 Coordinates for Blade Profile generation

| z _{pressure} (mm) | r _{pressure} (mm) | θ _{pressure} (rad) | z _{suction} (mm) | r _{suction} (mm) | θ _{suction} (rad) |
|----------------------------|----------------------------|-----------------------------|---------------------------|---------------------------|----------------------------|
| 0 | 3.85 | 0.055 | 0 | 3.85 | -0.055 |
| 0.45 | 3.92 | 0.166 | 0.45 | 3.92 | 0.068 |
| 0.91 | 3.99 | 0.26 | 0.91 | 3.99 | 0.172 |
| 1.36 | 4.07 | 0.339 | 1.36 | 4.07 | 0.261 |
| 1.82 | 4.14 | 0.404 | 1.82 | 4.14 | 0.336 |
| 2.27 | 4.22 | 0.458 | 2.27 | 4.22 | 0.4 |
| 2.72 | 4.31 | 0.502 | 2.72 | 4.31 | 0.453 |
| 3.17 | 4.41 | 0.537 | 3.17 | 4.41 | 0.497 |
| 3.62 | 4.53 | 0.566 | 3.62 | 4.53 | 0.533 |
| 4.06 | 4.66 | 0.588 | 4.06 | 4.66 | 0.562 |
| 4.49 | 4.82 | 0.605 | 4.49 | 4.82 | 0.585 |
| 4.91 | 5 | 0.617 | 4.91 | 5 | 0.603 |
| 5.32 | 5.21 | 0.627 | 5.32 | 5.21 | 0.616 |
| 5.71 | 5.46 | 0.633 | 5.71 | 5.46 | 0.626 |
| 6.08 | 5.74 | 0.637 | 6.08 | 5.74 | 0.633 |
| 6.42 | 6.05 | 0.64 | 6.42 | 6.05 | 0.637 |
| 6.72 | 6.39 | 0.641 | 6.72 | 6.39 | 0.64 |
| 6.99 | 6.77 | 0.642 | 6.99 | 6.77 | 0.641 |
| 7.23 | 7.16 | 0.642 | 7.23 | 7.16 | 0.642 |
| 7.43 | 7.58 | 0.642 | 7.43 | 7.58 | 0.642 |
| 7.59 | 8.01 | 0.642 | 7.59 | 8.01 | 0.642 |

Table 3.5 Turbine blade profile co-ordinates of pressure and suction surfaces

Computational flow analysis

4. Computational fluid flow analysis

The computational flow analysis of a cryogenic turboexpander is done in three steps. The turbine model is created in bladegen by using the data available for hub, shroud and blade profile. The meshing of the turbine is done in turbogrid. Simulation settings and other physical parameters are defined and specified in CFX-Pre. This is required to describe the flow conditions at inlet and outlet of the turboexpander. The examining and study of the result are done in CFX-Post.

4.1 Design of expansion turbine in bladegen

A geometry creation tool i.e. ANSYS Bladegen is used for designing the blades. This tool is specialised for creating turbomachinery blades. The modelling of the blade in bladegen is done using the available coordinates of hub, shroud and blade profile. The coordinates of the hub and tip profile are given in the previous chapter. The hub and tip profile are joined with a number of tie lines, through which a surface is created. The blade surface so created is lofted in the blade editor by curve that goes from hub to shroud. The surface generated is known as the mean surface of the blade. Solid surface are developed by using the non-Uniform Rational B Splines. The pressure and suction surface of two contiguous channel are calculated by finding the mean surface in the direction of positive and negative theta through half blade thickness.

After the creation of all surfaces, the blade merging topology is used. This property merges all the blade faces that are tangent to each other. Create fluid zone property is selected, to create a stage fluid zone body for the flow passage, and an enclosure feature to subtract the blade body. This leading enclosure can be employed for a CFX analysis of the blade transition. "Create all blades" option is used to input the number of blades required for the bladegen model. Here we input number of blade as ten.

Different views of radial turbine in bladegen are as following:

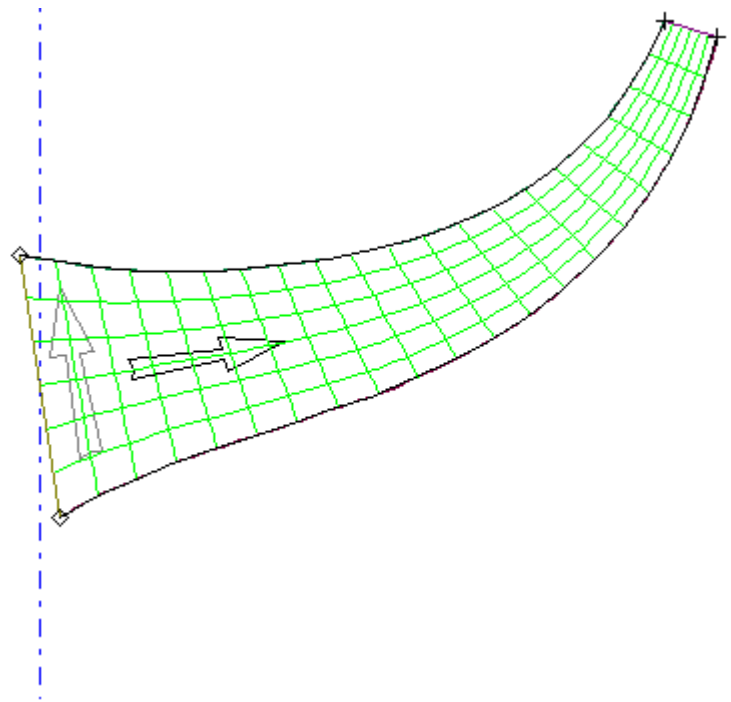


Figure 4.1 Meridional blade profile

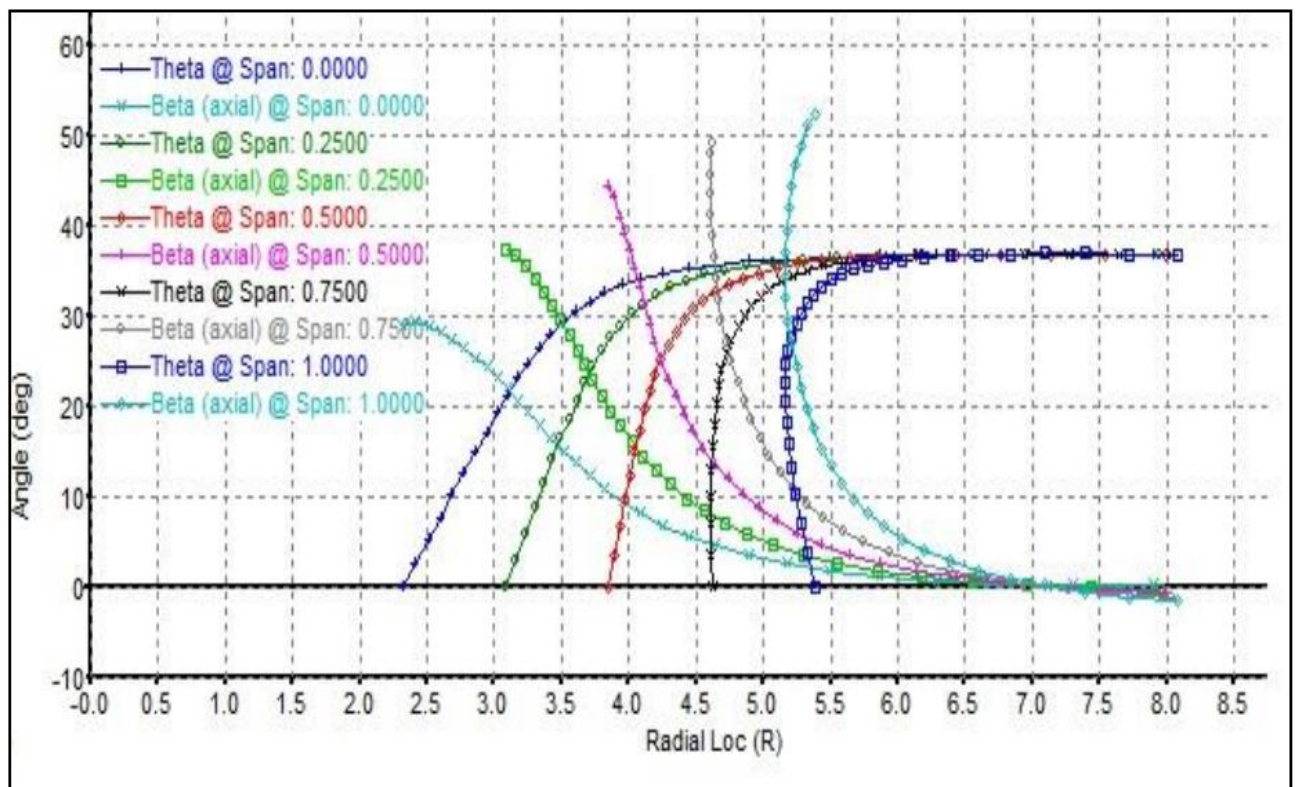


Figure 4.2 Variation of Beta and Theta at different spans

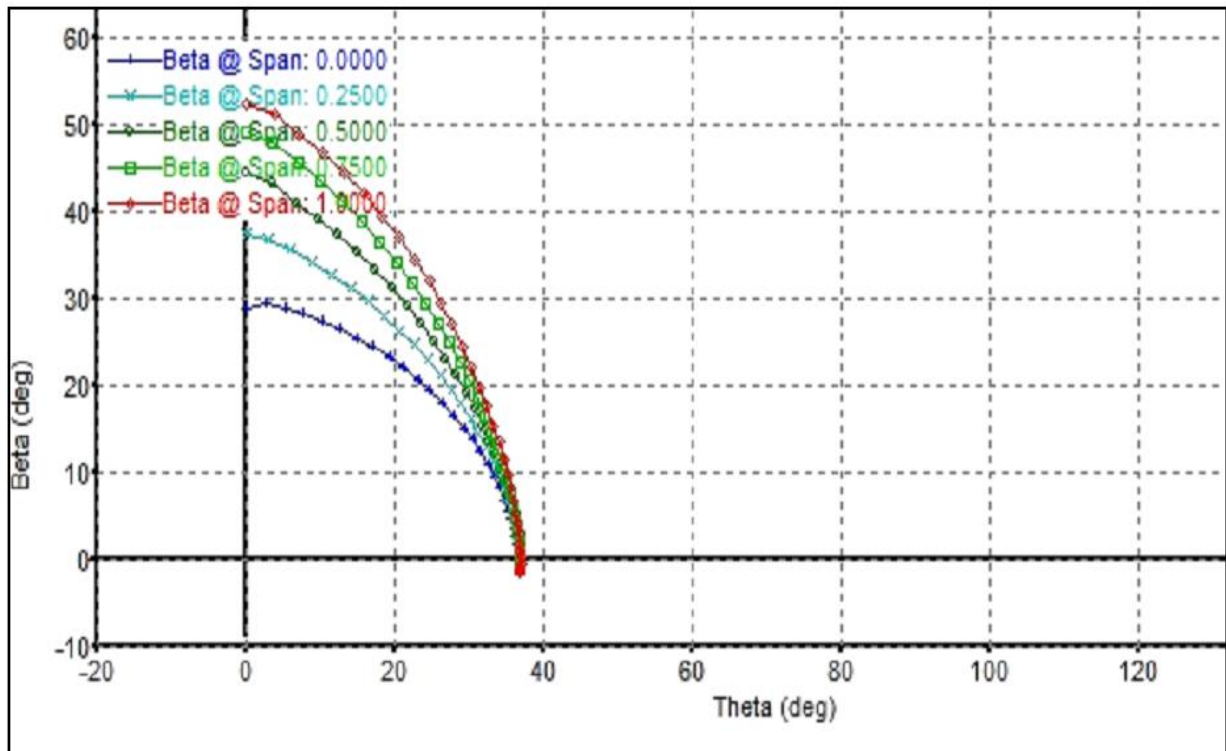


Figure 4.3 Variation of Beta and Theta

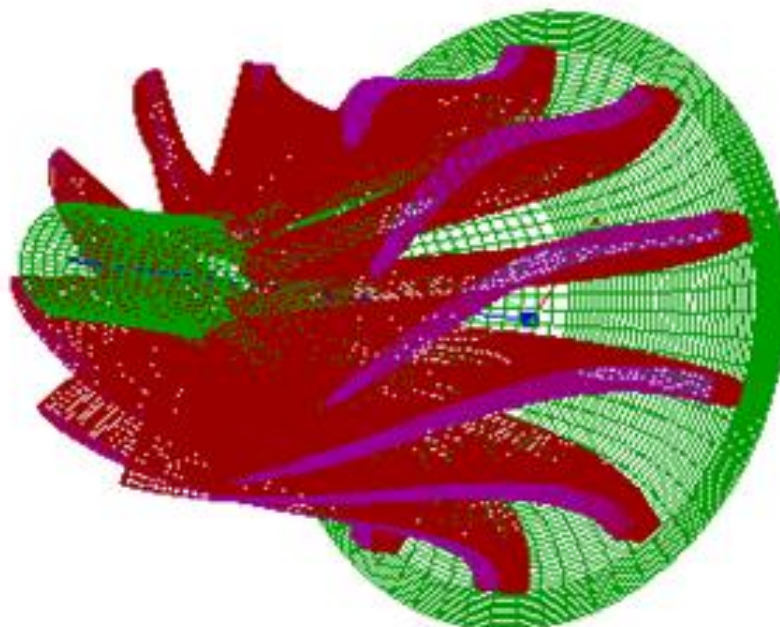


Figure 4.4 Wireframe model of turbine generated in bladen

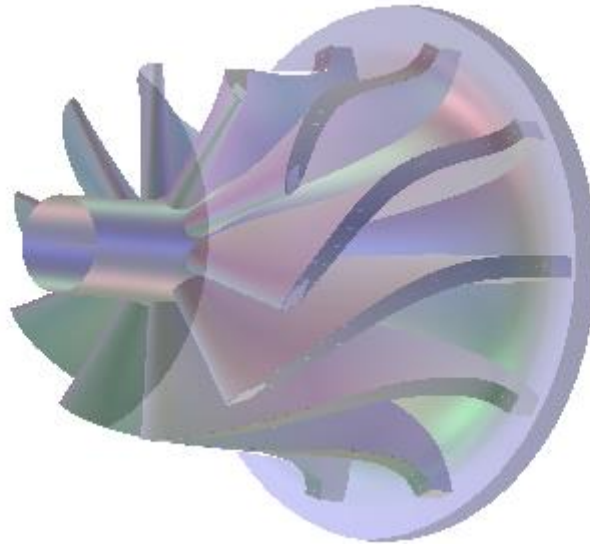


Figure 4.5 Solid model of turbine in bladegen

4.2 Meshing of the turbine model

Turbogrid is used for the meshing of the turbine model. For the demands of fluid flow analysis of turbine rotor, turbogrid creates a high grade of hexahedral meshes. The turbine model data is imported from the bladegen. The turbine rotor data file imported from bladegen is used by turbogrid to set the rotational axis, total number of blade and length unit for scaling of machine. The primary information about the geometry is provided by the machine data. The units specified here for base unit represents the scale of geometry which is being meshed. These units do not control the unit that are associated to mesh file neither they are utilised for the import of geometric data, they are only employed for internal representation of turbine model to limit the computer round off errors. A 1 mm gap is provided between the blade and shroud, this completes the geometry.

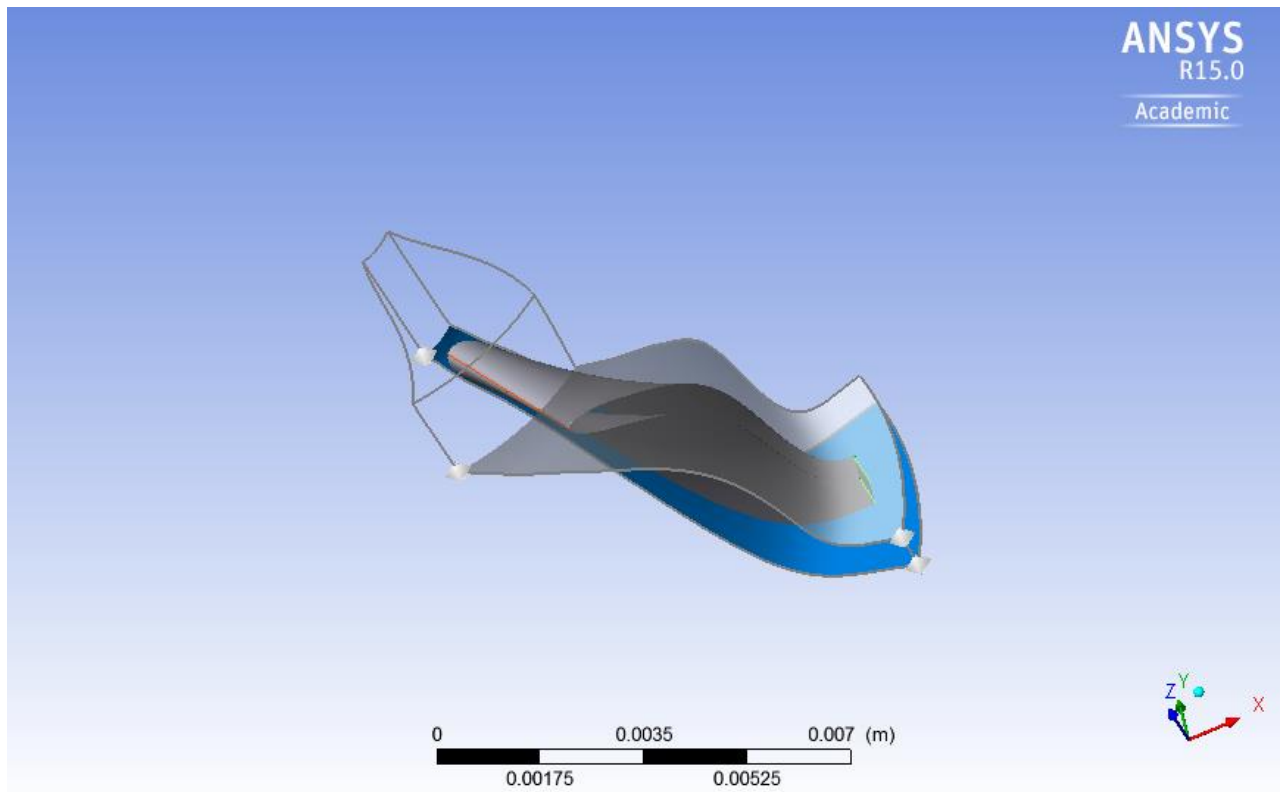


Figure 4.6 view of turbine blade after bladen import

The following step is for generating the topology that helps in guiding the mesh. The access to the topology legacy method and is provided by topology definition and placement to traditional with control points. The H/J/C/L-Grid technique makes ANSYS Turbogrid to select one of the grid method or the combination of the grid methods based on certain rules. In this circumstance, the H/J/C/L-Grid technique makes ANSYS Turbogrid to select a H-Grid topology for upstream end passage, and a H-Grid topology for downstream end passage. There is also an O-Grid selection with a width factor of 0.5. The O-Grid (which is thickness half the mean blade thickness) is selected to enhance the mesh orthogonality in the region.

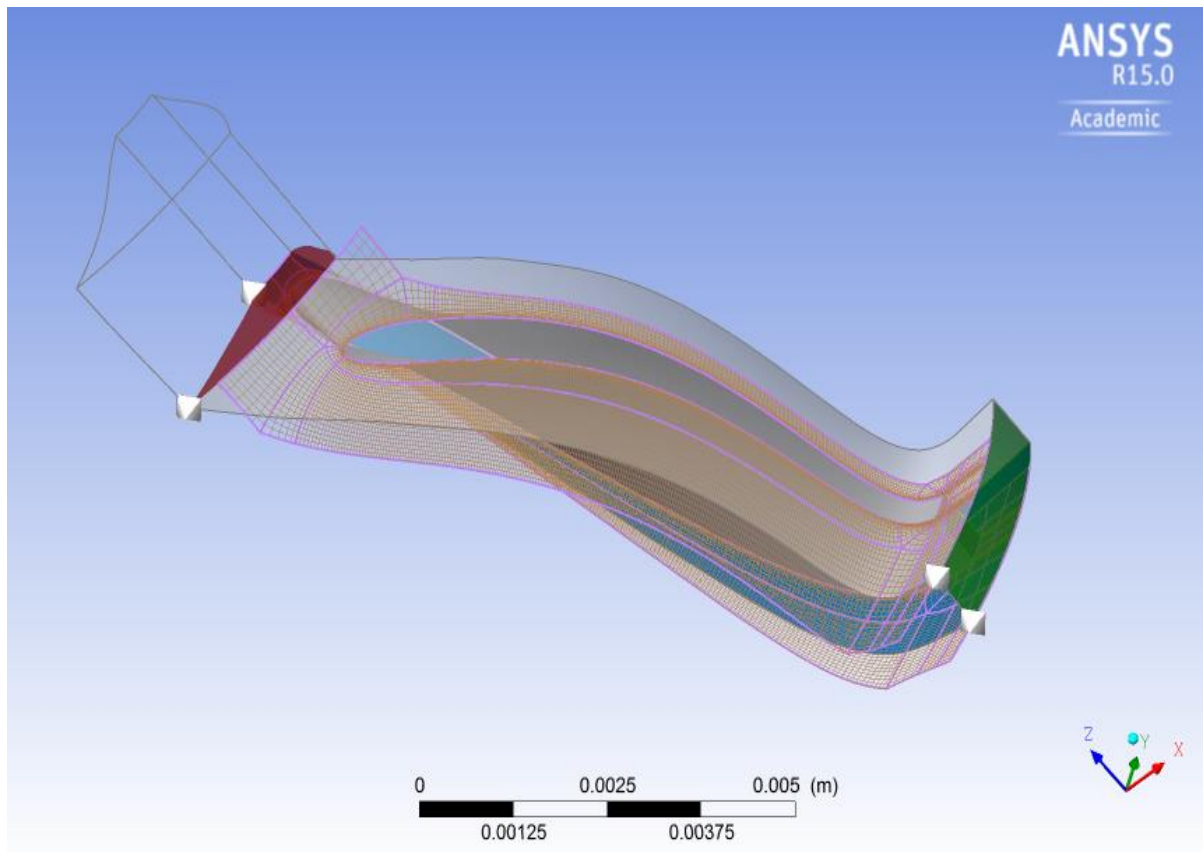


Figure 4.7 view of the turbine rotor after mesh topology is set

After the topology is defined, the setting of mesh data is done to govern the number of mesh element and distribution of these elements. In this case, to generate a fine mesh the target number of nodes is set to 250000. The 3D mesh is generated after the mesh quality is verified on the layers, particularly the layers at hub and the shroud tip. After the correction of mesh accuracy on layers, the mesh with 206178 elements and 228410 node is generated.

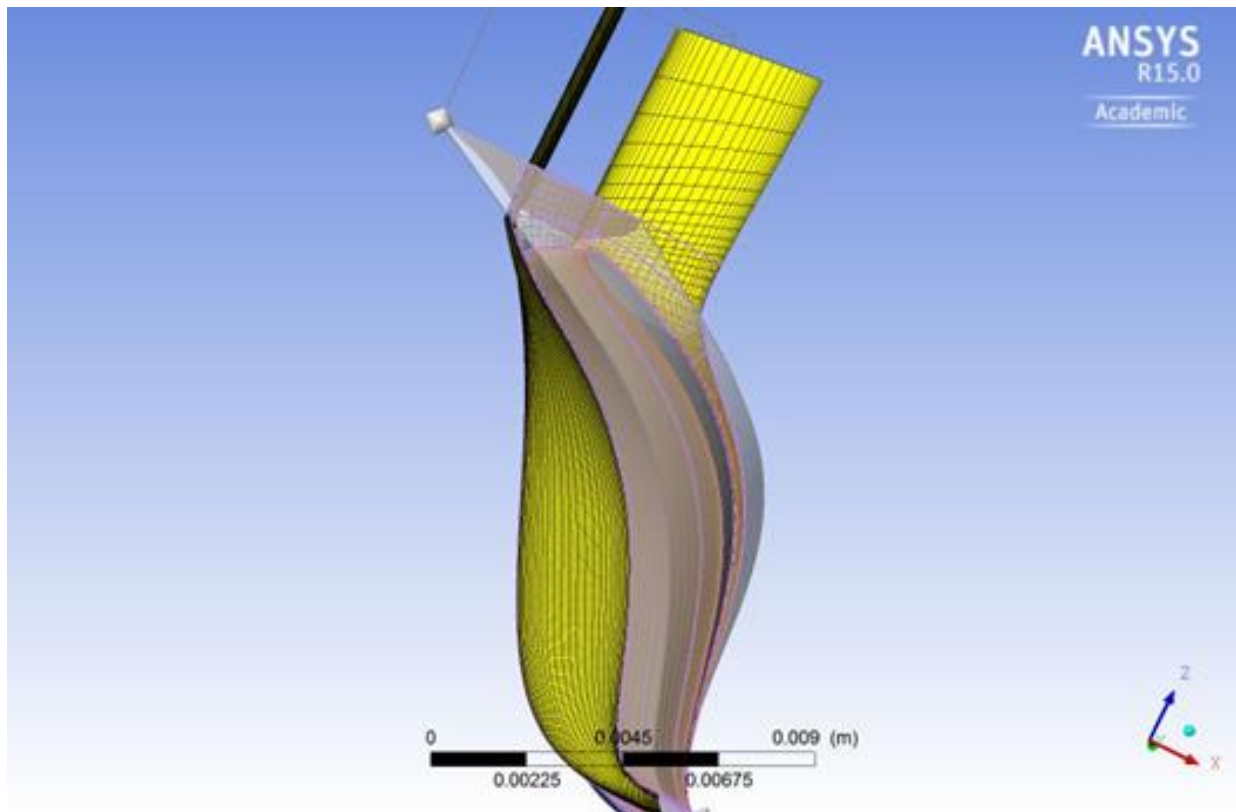


Figure 4.8 view of the turbine blade after meshing

4.3 Physic definition of meshed model in CFX-Pre

CFX-Pre is considered as physic definition pre-processor of ANSYS CFX. The physic definition of the meshed turbine rotor is done in CFX by using the turbo mode. Under general setting of turbo mode the type of machine is defined as radial turbine and z axis is selected as the rotational axis. In component definition option we choose the component type as rotating and give the rotational value as 218780 rev/min. Turbo mode automatically detects different regions that represent to some boundary types. This data should be analysed in Region Information section to assure that everything is precise. This information helps in setting up boundary condition and interfaces. In the wall configuration tab we set the tip clearance at shroud. In the physic definition tab we set the type of fluid, model data type of analysis to be done, inflow and outflow boundary conditions and solver parameter.

| Tab | Setting | | Values |
|------------|-----------------------------------|---------------------|------------------------------------|
| Physics | Fluid | | Nitrogen |
| Definition | Analysis Type | | Steady state |
| | Modal Data | Reference pressure | 0 (Pa) |
| | | Heat Transfer | Total Energy |
| | | Turbulence | k-Epsilon |
| | Inflow/Outflow Boundary Templates | | Mass Flow Inlet P-Static Outlet |
| | Inflow | T-Total | 99.65k |
| | | Mass Flow | Per Component |
| | | Mass Flow Rate | 0.002326 kg/sec |
| | | Flow Direction | Normal to Boundary |
| | Outflow | P-Static | 1.29 bar |
| | Solver Parameters | Advection Scheme | High Resolution |
| | | Convergence control | Physical Timescale |
| | | Physical Timescale | 0.000004 s |

Table 4.1 Physic definition input for turbine rotor

After the physic definition input CfX-Pre will create precise boundary condition and interface with the help of region names which were provided antecedently in region information.

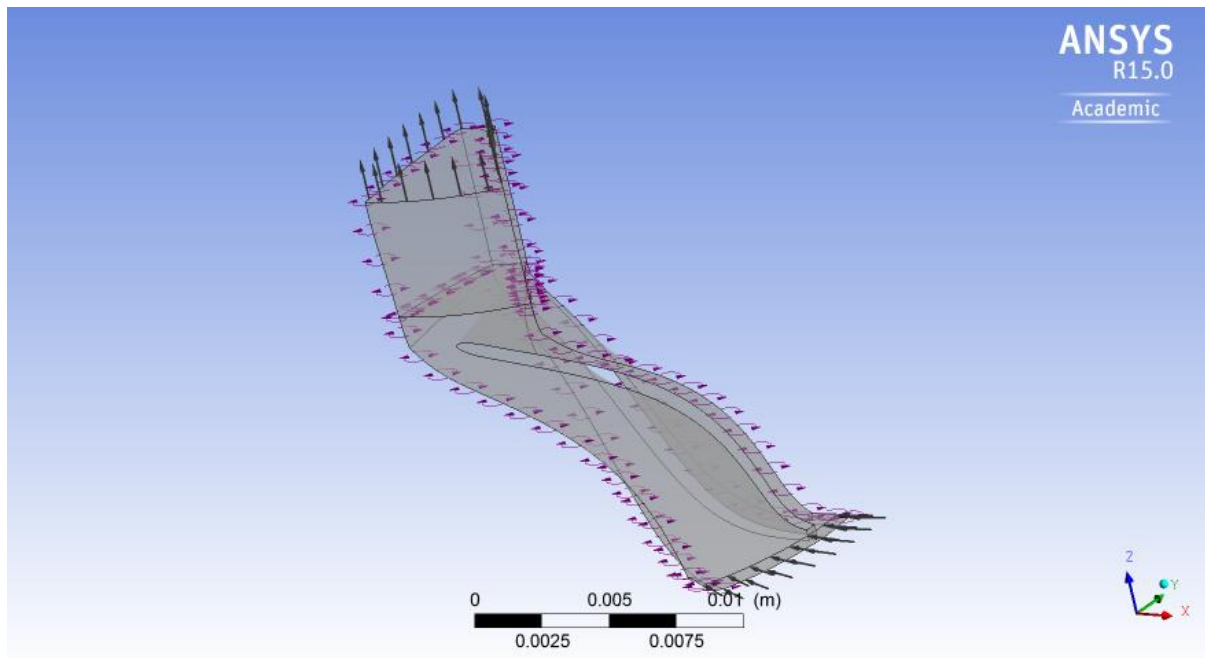


Figure 4.9 direction of flow at inlet and outlet

4.4. The solution of the flow by means of CFX solver

This chapter gives the detail about the mathematical equations used for the fluid flow model, heat and mass transfer for single phase, single or multi component flow without radiation or combustion in ANSYS CFX.

ANSYS CFX compute for relative static pressure inside the flow field which depends upon the absolute pressure.

$$P_{abs} = P_{ref} + P_{stat}$$

Specific static enthalpy is the amount of energy per unit mass contained in a fluid. Static enthalpy is related to internal energy of the fluid and fluid state:

$$h_{stat} = u_{stat} + (P_{stat} / \rho_{stat})$$

By using the thermal energy model, the CFX-solver directly calculates the static enthalpy.

The equations that are calculated by ANSYS CFX are unsteady navier stokes equation in its conservation form. The conservation equations of mass, momentum and energy are given below in stationary frame:

Continuity equation $\frac{\partial \rho}{\partial t} + \nabla \cdot (\rho \vec{v}) = S_m$

Momentum equation $\frac{\partial(\rho \vec{v})}{\partial t} + \nabla \cdot (\rho \vec{v} \vec{v}) = -\nabla p + \nabla \cdot (\vec{\tau}) + \rho \vec{g} + \vec{F}$

Where stress tensor τ depends upon strain rate by

$$\tau = \mu \left(\nabla U + (\nabla U)^T - \frac{2}{3} \delta \nabla \cdot U \right)$$

Total energy equation $\frac{\partial(\rho h_{tot})}{\partial t} - \frac{\partial P}{\partial t} + \nabla \cdot (\rho U h_{tot}) = \nabla \cdot (\lambda \nabla T) + \nabla \cdot (U \cdot \tau) + U \cdot S_M + S_E$

Where total enthalpy h_{tot} depends upon static enthalpy $h(T, P)$ by

$$h_{tot} = h + \frac{1}{2} U^2$$

The term $U \cdot S_M$ gives the work caused by external momentum and it is presently neglected.

CFX Solver simultaneously runs the solver and monitors the output. The input file of CFX Solver is generated by ANSYS Workbench and after that it forwards it to ANSYS CFX-Solver. First of all the solution unit in CFX Solver is set as SI unit. In the solution control tab, maximum number of iteration is set to 10000 and the residual type is set to RMS. Convergence criteria and residual is targeted as 1.E-4. In the output control the output variable is set to temperature.

When the define run panel appears, the solver input file is automatically set by ANSYS. After that the solver run is started. After the completion of solver run a dialog box appears giving a completion message.

4.5. Obtaining Results in CFX-Post:

CFX-Post is a versatile post processor. It allows the user for a clear visualisation and a valued analysis of result obtained in CFD simulations. It includes all kind of plotting such as iso surface, streamlines, animations, contours, vectors etc.

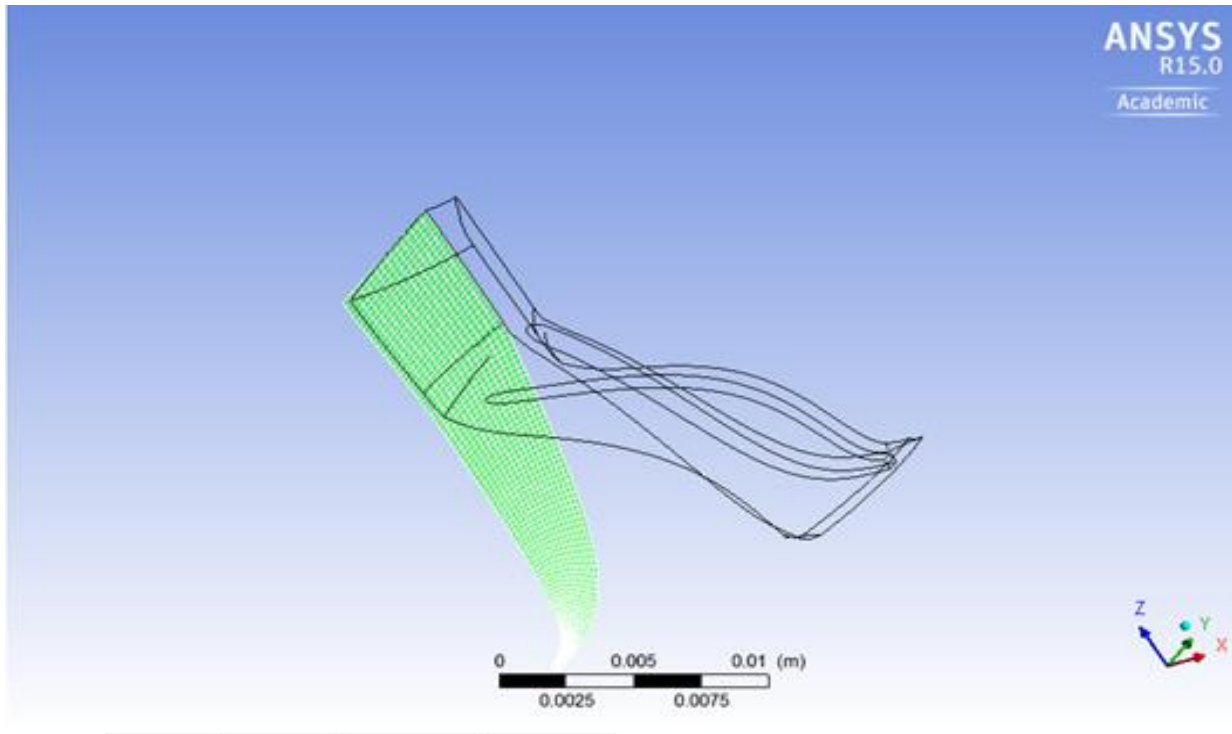


Fig 4.10 Wireframe and Meridional model of turbine rotor

Chapter 5

Result and discussion

5. Result and discussion

The analysis of the computational fluid flow is carried out in CFX Post after simulation in CFX is completed. A tabularised result can be visualised in following report. This report provides the change in thermodynamic properties from hub to shroud and from inlet to outlet.

Change in thermodynamic properties at different regions of turbine rotor is provided in the table

| Quantity | Inlet | outlet | Unit |
|------------|---------|---------|---------------------------------------|
| Density | 8.5642 | 4.4334 | [Kg m ⁻³] |
| Pstatic | 253267 | 135429 | [Pa] |
| Ptotal | 313127 | 178920 | [Pa] |
| Tstatic | 95.5492 | 88.7354 | [K] |
| Ttotal | 99.3427 | 96.7352 | [K] |
| Entropy | 5357.2 | 5632.16 | [J kg ⁻¹ K ⁻¹] |
| Mach (abs) | 0.772 | 0.6012 | |
| Mach (rel) | 1.2632 | 0.8632 | |
| U | 186.88 | 130.14 | [m s ⁻¹] |

Table 5.1: variation of thermodynamic properties

From the above table, it is seen that within the turbine pressure, velocity mach number, temperature and density keeps on decreasing from inlet to outlet while the entropy increases from inlet to outlet. Static temperature found out at outlet is 88.73K which is approximately the temperature obtained by S. K. Ghosh [52] while experimenting on turboexpander.

Therefore the output obtained is validated to the result obtained by S.K. Ghosh [52] experimentally.

Different graphs and contour plotted from the results are as following:

5.1 streamwise variation of pressure from inlet to outlet

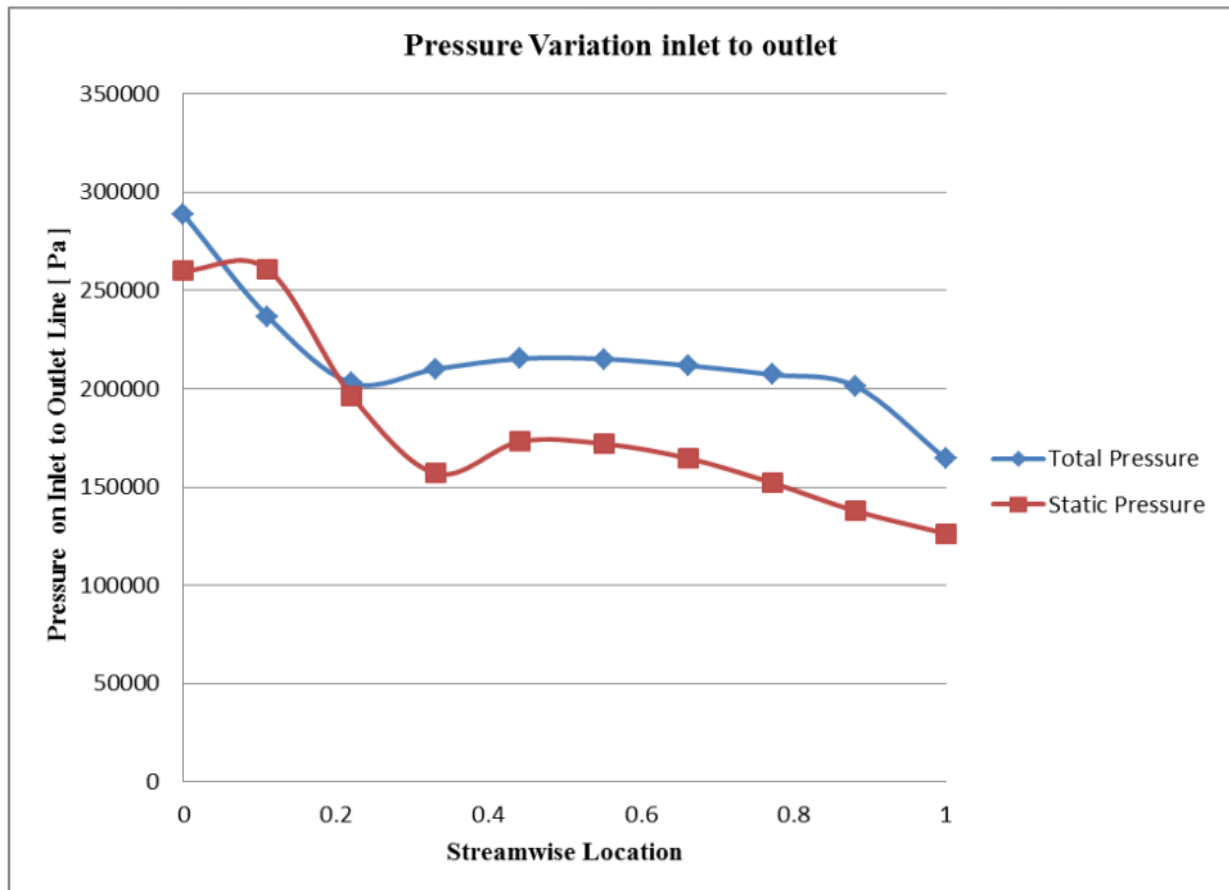


Figure 5.1 variation of pressure from inlet to outlet

The streamwise variation of static and total pressure from inlet to outlet is provided in the above graph. Total pressure at inlet is nearly 3 bar while at outlet it is 1.7 bar. The static pressure at inlet is 2.5 bar and at outlet is 1.3 bar. This value obtained is nearly equal to the result found out by S.K. Ghosh [52].

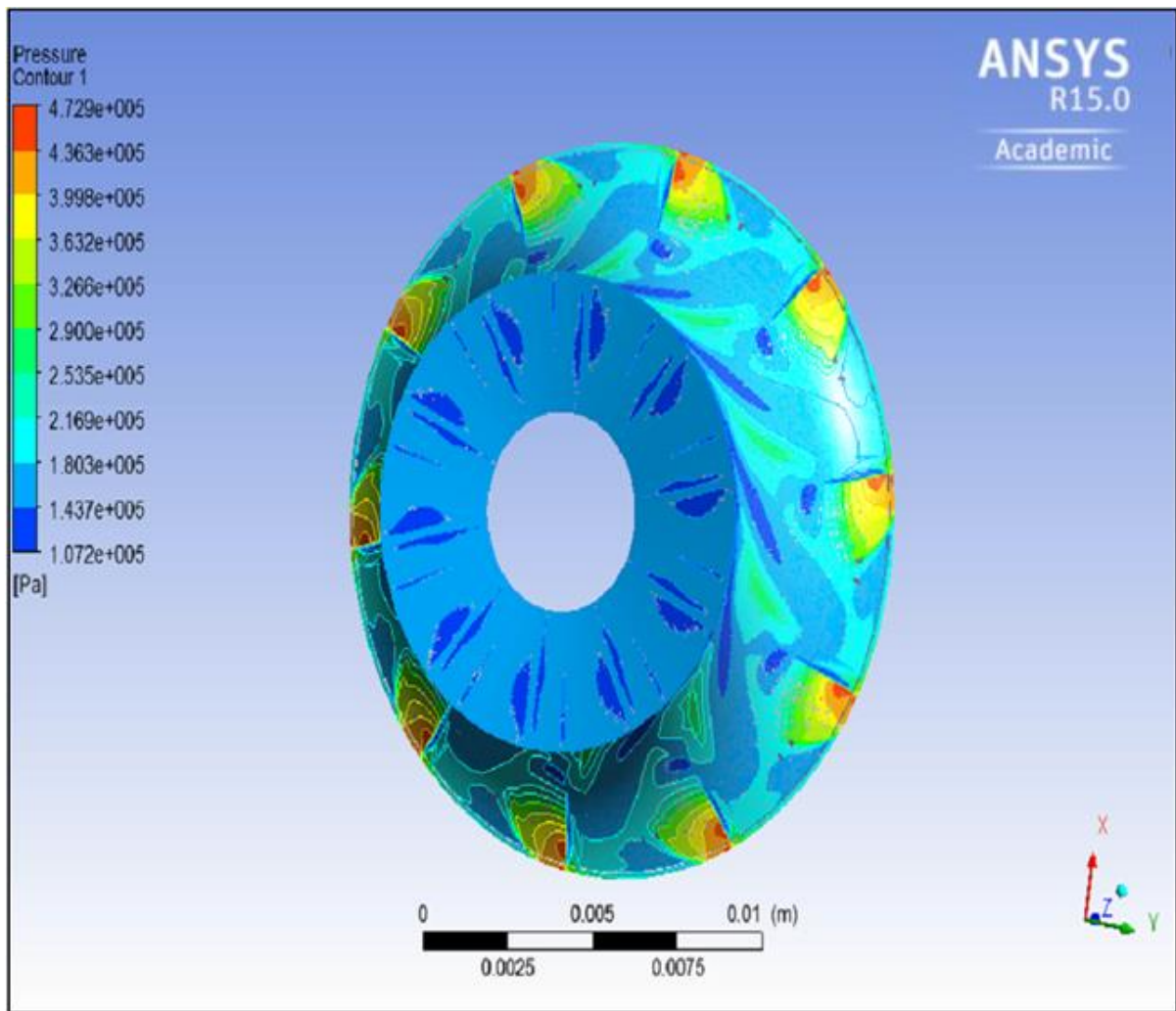


Figure5.2 Isometric view of pressure variation

5.2 Streamwise variation of temperature from inlet to outlet:

The streamwise variation of static and total temperature from inlet to outlet is provided in the graph below. Total temperature at inlet is 99.34 K while at outlet it is 96.73 K. The static temperature which is 95.54 at inlet decreases to 88.73 K at outlet. This value obtained is nearly equal to the result found out by S.K. Ghosh [52].

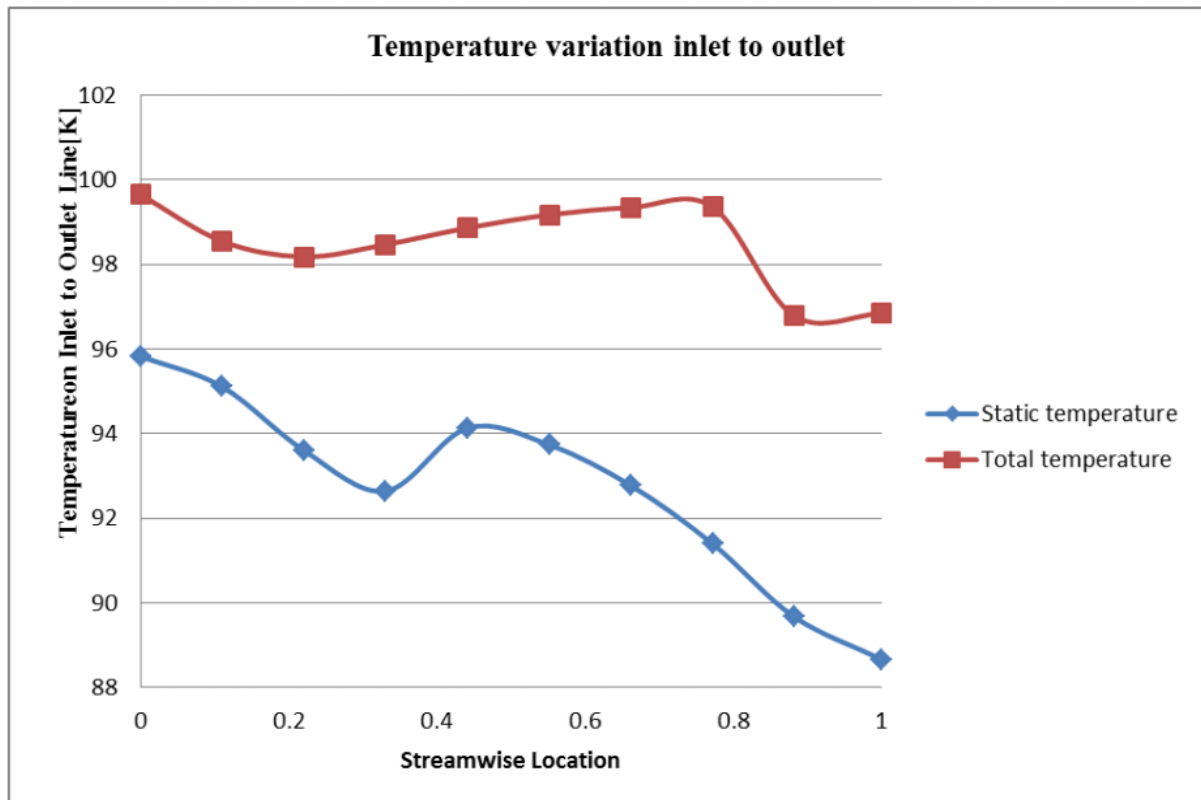


Figure 5.3 Temperature variation along streamwise inlet to outlet

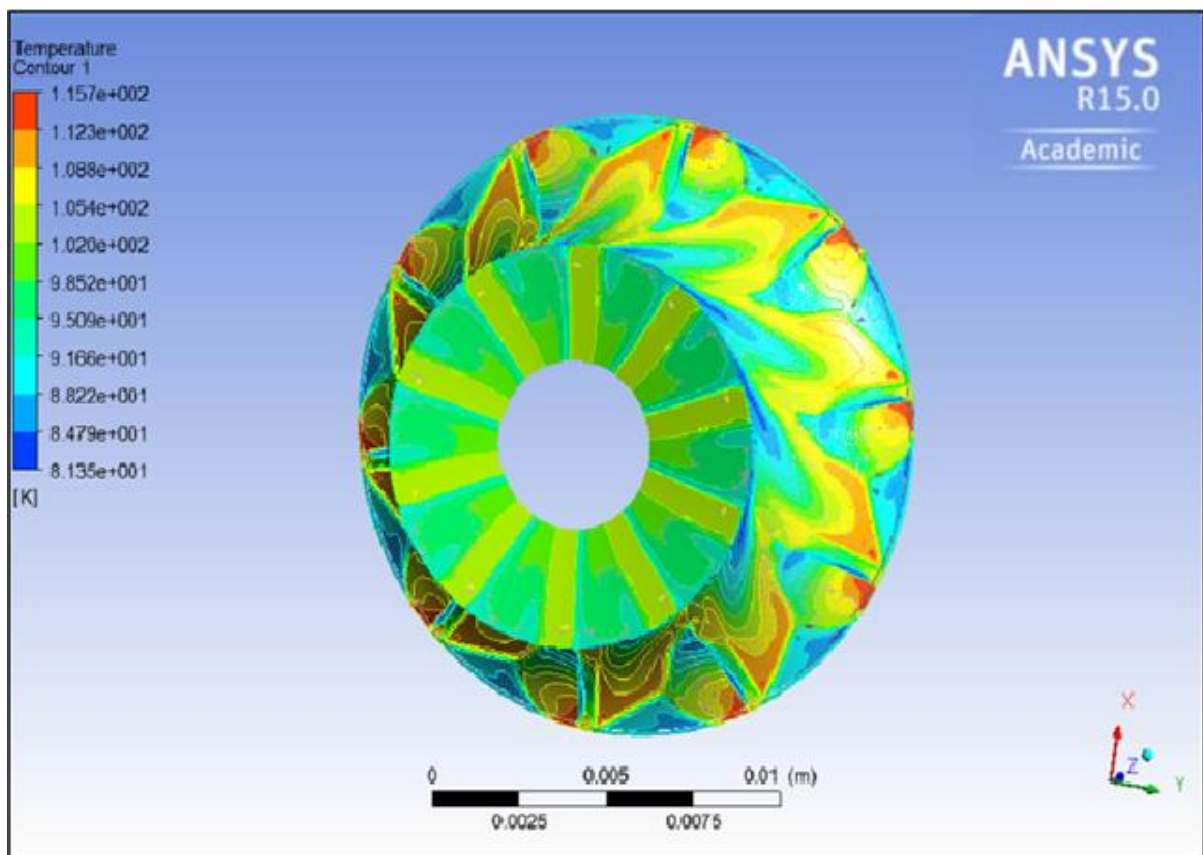


Figure 5.4 Isometric 3D view of temperature variation

5.3 Streamwise variation of velocity from inlet to outlet:

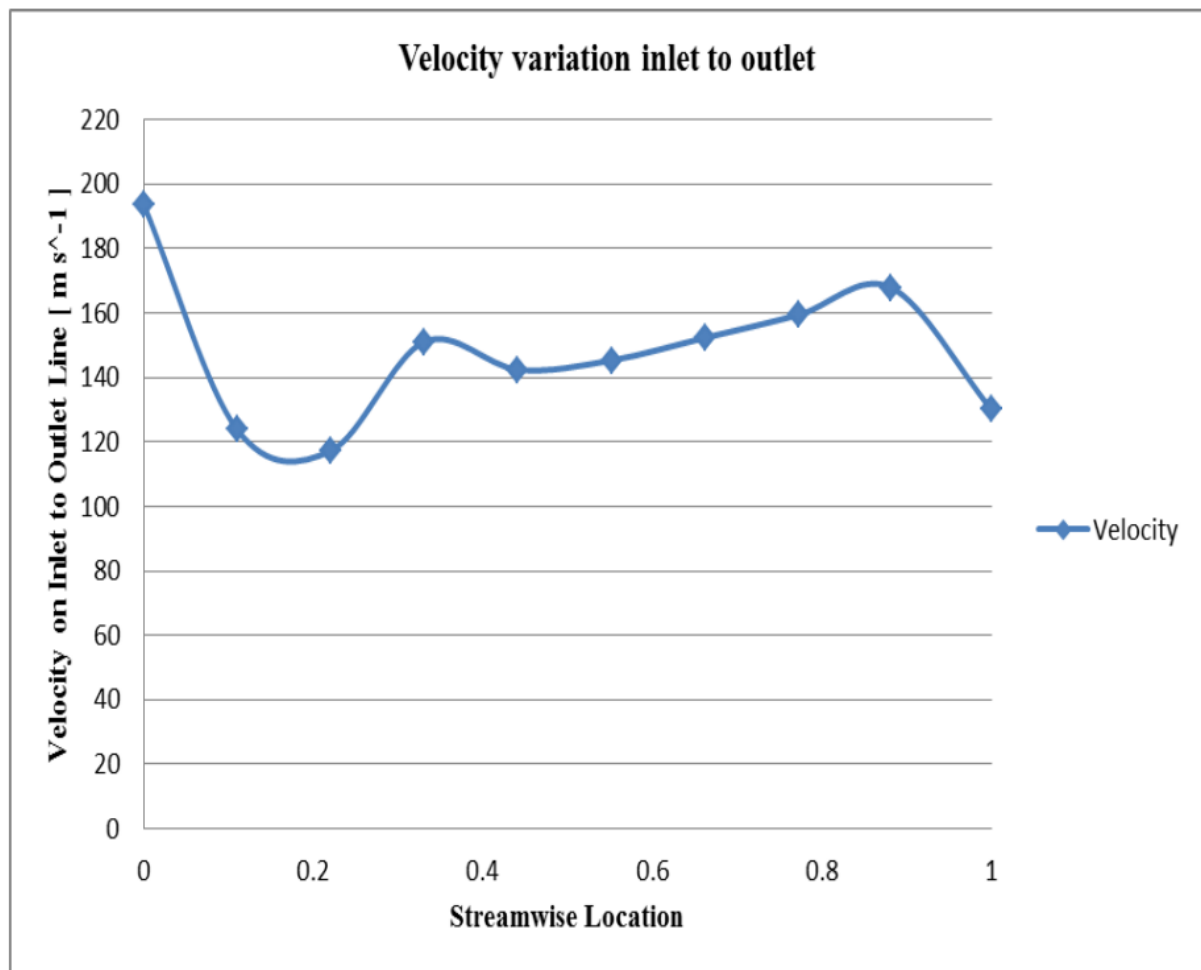


Figure 5.5 Variation of velocity from inlet to outlet

The streamwise variation of velocity from inlet to outlet is provided in the above graph. The velocity decreases from inlet to outlet. At the inlet the velocity is 186.88 m/s while at the outlet it is 130.14 m/s.

5.4 Streamwise variation of Mach number

The streamwise variation of absolute and relative Mach number is observed in the graph below. Absolute Mach number varies from inlet to outlet as 0.772 to 0.6. Relative Mach number decreases from 1.3 to 0.8.

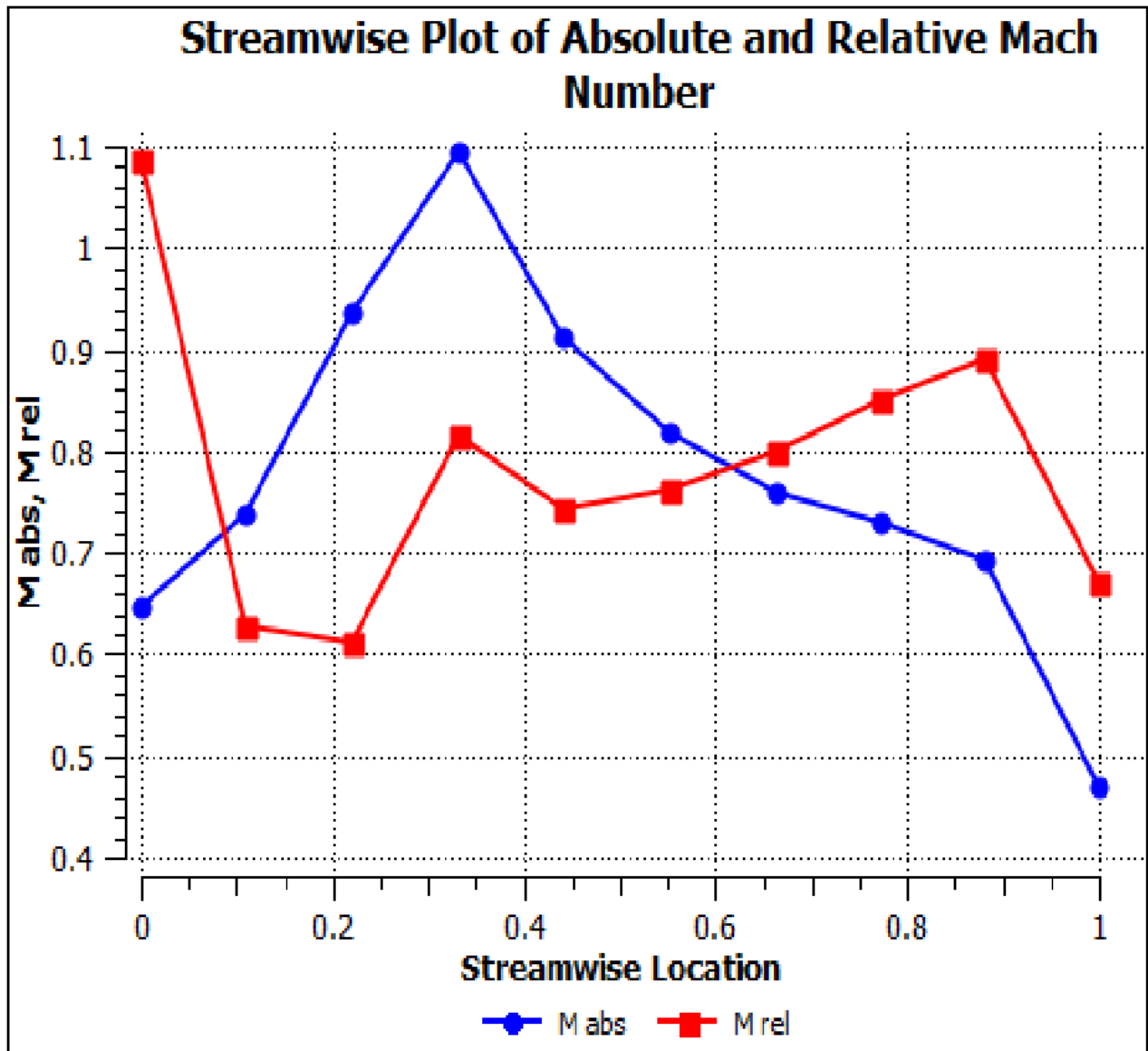


Figure 5.6 Streamwise variation of Mach number

5.3 Variation of density from inlet to outlet:

The streamwise variation of density from inlet to outlet is provided in the graph below. Density inside the turbine decreases from inlet to outlet. Density at inlet is 8.564.43 Kg/m³ whereas at outlet it is 4.43 Kg/m³.

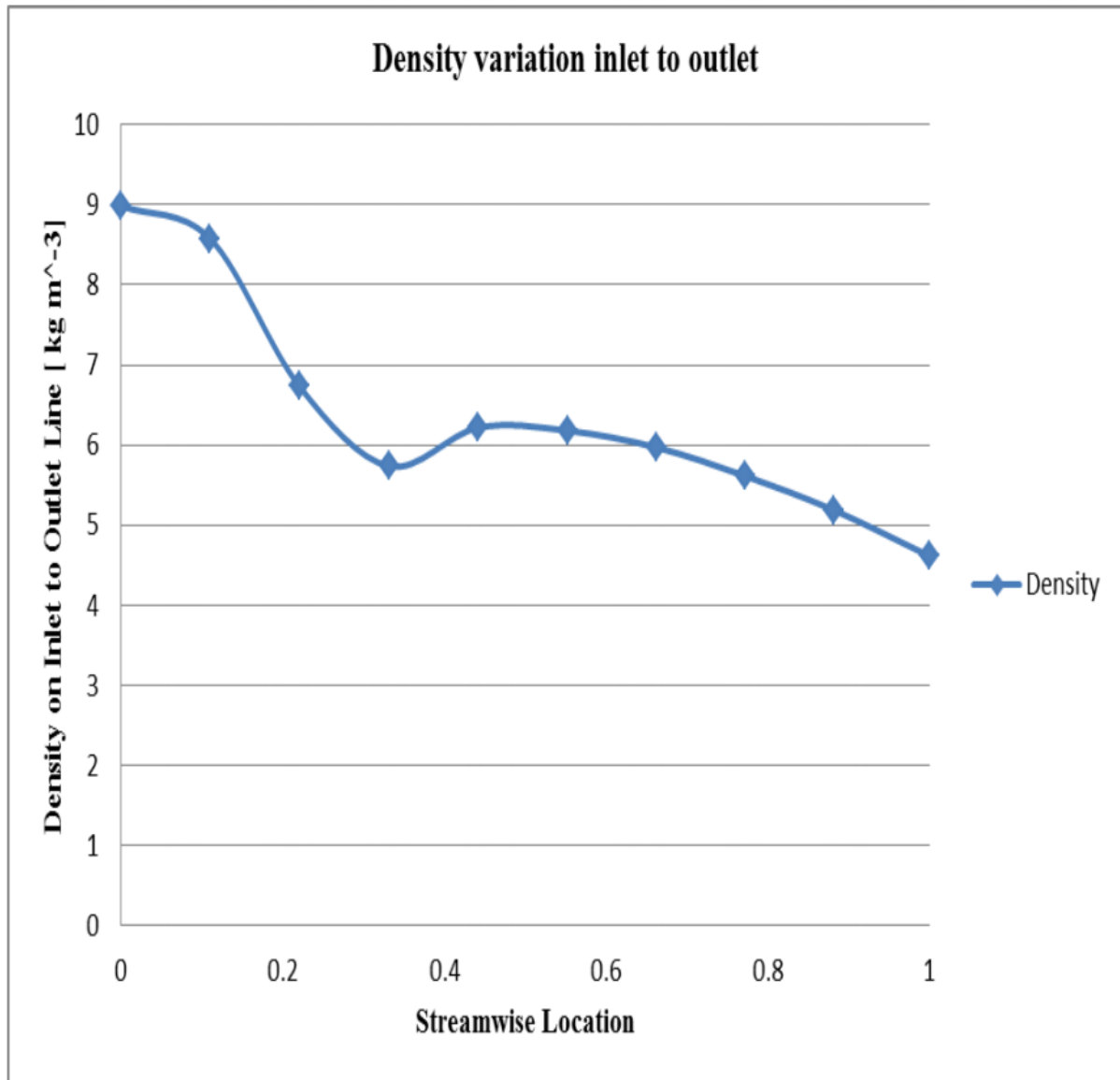


Figure 5.7 Variation of density from inlet to outlet

5.6 Streamwise variation of Entropy

The streamwise variation of entropy from inlet to outlet is provided in the graph below. At the inlet the value of entropy is $5357.2 \text{ J kg}^{-1}\text{K}^{-1}$ whereas at the outlet the value of entropy is $5632.16 \text{ J kg}^{-1}\text{K}^{-1}$. It is seen that entropy increases from inlet to outlet inside the turbine.

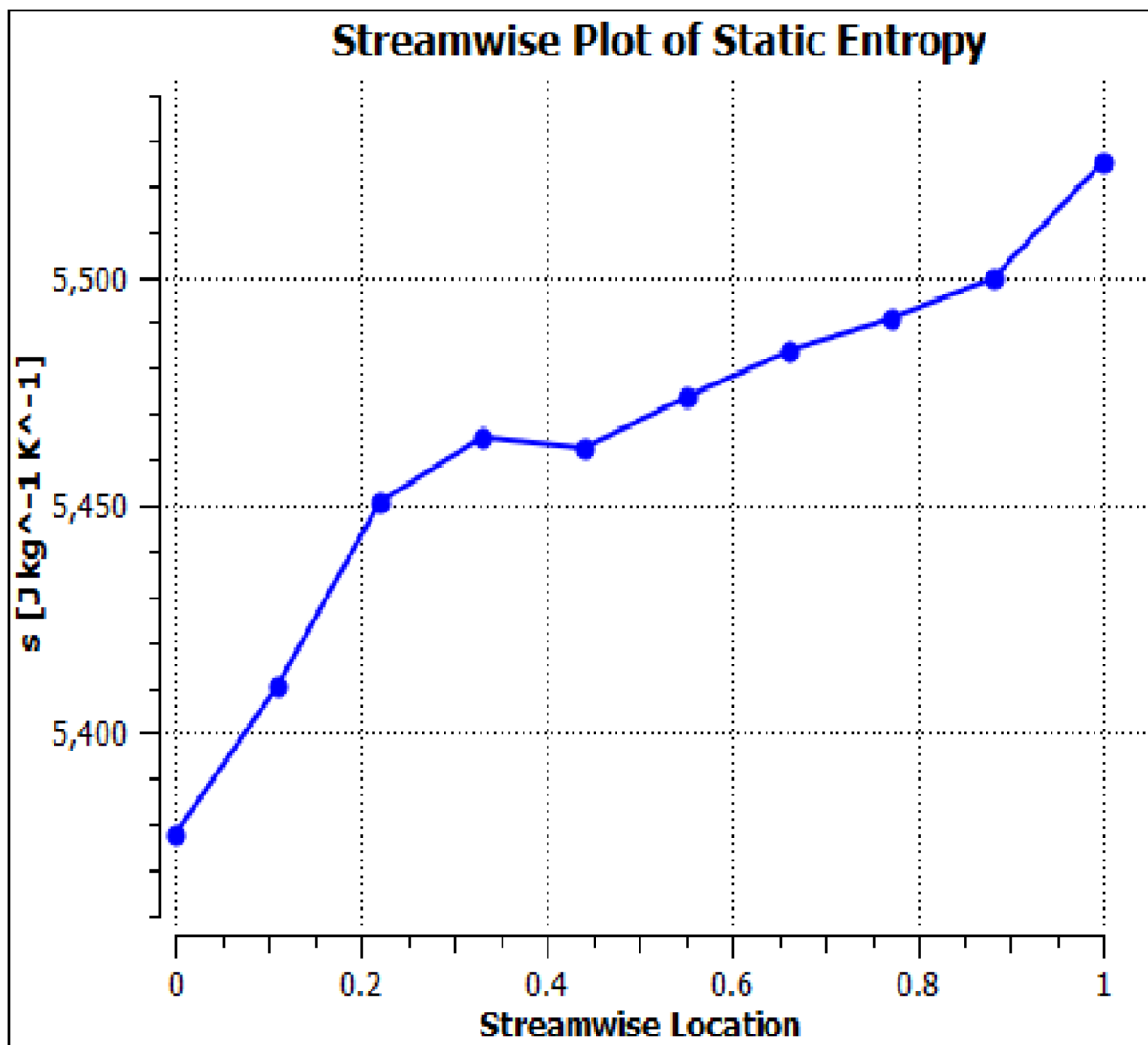


Figure 5.8 Streamwise variation of Entropy

5.7 Streamline variation at trailing edge of the blade

It is observed in fig. 5.8 that at the trailing edge the colour of streamline changes to blue, which means that there is a decrease in velocity of the fluid.

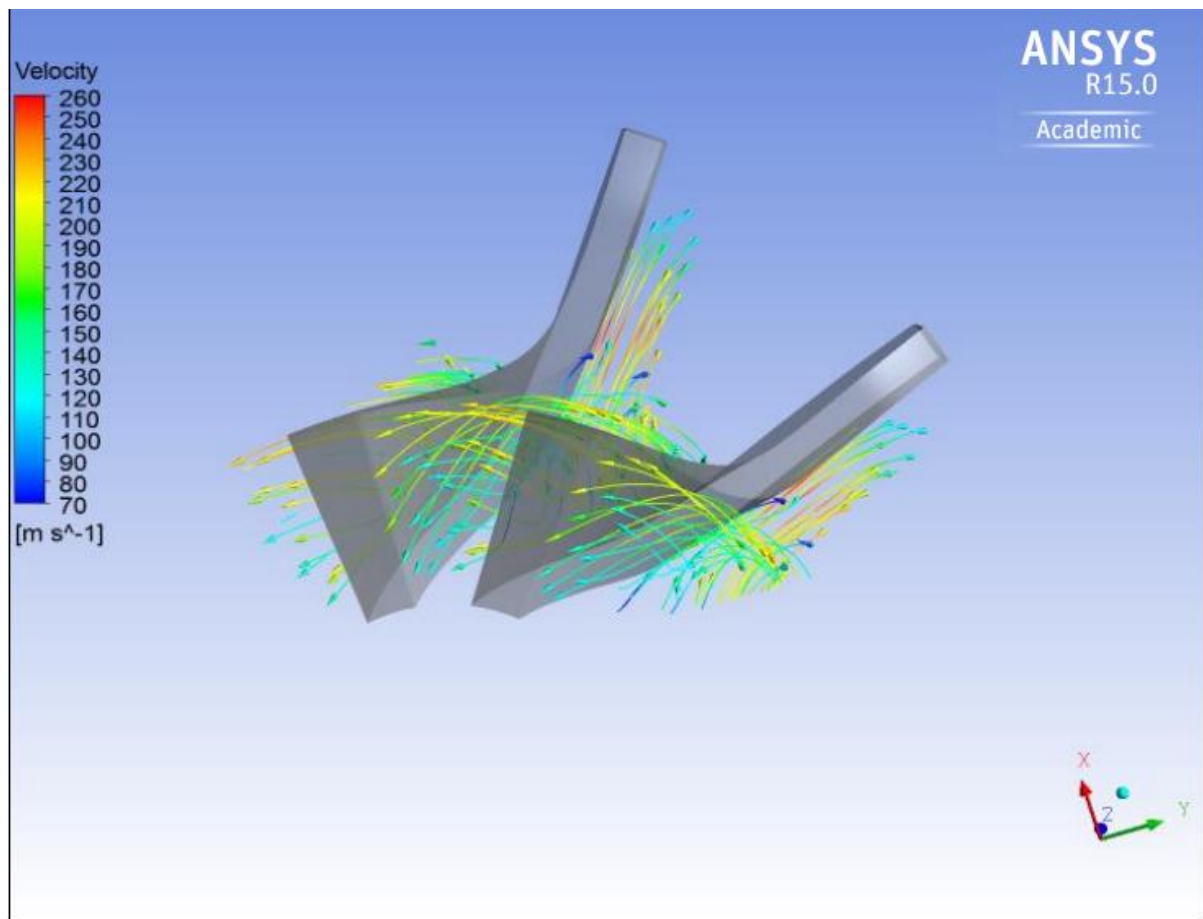


Figure 5.9 Streamline variation at trailing edge of the blade

Chapter 6

Conclusion and future work

Conclusion and future work

6.1 Conclusion

A modest attempt has been made for analysing the flow inside a cryogenic turboexpander using computational flow dynamic method. An expansion turbine model is designed, meshing of the model was done and the simulation was performed. The modelling of the expansion turbine was done by designing the hub, shroud and blade profile in bladegen. The turbine model was meshed in turbogrid and after that the computational flow analysis was done in CFX. By validating the result with experimental values various graphs and contours of different thermodynamic properties were plotted.

6.2 Future work

Future work should be in the direction of computational flow analysis of other parts of the turboexpander such as nozzle, diffuser etc. A complete turboexpander model can be analysed by a proper simulation.

References:

- [1] **Collins, S.C. and Cannaday, R.L.** Expansion Machines for Low Temperature Processes
Oxford University Press (1958).
- [2] **Sixsmith, H.** Miniature cryogenic expansion turbines - a review Advances in Cryogenic
Engineering (1984), V29, 511-523.
- [3] **Swearingen, J. S.** Turbo-expanders Trans AIChE (1947), 43 (2), 85-90
- [4] **Clarke, M. E.** A decade of involvement with small gas lubricated turbine & Advances in
Cryogenic Engineering (1974), V19, 200-208
- [5] **Beasley, S. A. and Halford, P.** Development of a High Purity Nitrogen Plant using
Expansion Turbine with Gas Bearing Advances in Cryogenic Engineering (1965),
V10B, 27-39
- [6] **Swearingen, J. S.** Engineers' guide to turboexpanders RotoFlow Corp, USA, (1970), Gulf
Publishing Company
- [7] **Voth, R. O., Norton, M. T. and Wilson, W. A.** A cold modulator refrigerator
incorporating a high speed turbine expander Advances in Cryogenic Engineering
(1966), V11, 127-138
- [8] **Colyer, D. B.** Miniature cryogenic refrigerator alternators Advances in Cryogenic
Engineering (1968), V13, 405-415
- [9] **Colyer, D. B. and Gessner, R. L.** Miniature cryogenic refrigerator Turbomachinery
Advances in Cryogenic Engineering (1968), V13, 484-493
- [10] **Sixsmith, H.** Miniature expansion turbines, C A Bailey (Ed), Advanced Cryogenics
Plenum Press (1971), 225-243
- [11] **Schmid, C.** Gas bearing turboexpanders for cryogenic plant 6th International Gas
Bearing Symposium University of Southampton England (March 1974) Paper 131 B1:
1-8

- [12] **Reuter K. and Keenan B. A.** Cryogenic turboexpanders with magnetic bearings AICHE Symposium Series, Cryogenic Processes and Machinery 89 (294), 35-45
- [13] **Izumi, H., Harada, S. and Matsubara, K.** Development of small size Claude cycle helium refrigerator with micro turbo-expander Advances in Cryogenic Engineering (1986), V31, 811-818
- [14] **Kun, L. C. and Hanson, T. C.** High efficiency turboexpander in a N₂ liquefier AICHE Spring meeting, Houston, Texas (1985)
- [15] **Kun, L. C.** Expansion turbines and refrigeration for gas separation and liquefaction Advances in Cryogenic Engineering (1987), V33, 963-973
- [16] **Kun, L. C. and Sentz, R. N.** High efficiency expansion turbines in air separation and liquefaction plants International Conference on Production and Purification of Coal Gas & Separation of Air, Beijing, China (1985), 1-21
- [17] **Sixsmith, H., Valenjuela, J. and Swift, W. L.** Small Turbo-Brayton cryocoolers Advances in Cryogenic Engineering (1988), V34, 827-836
- [18] **Creare Inc, USA** www.creare.com
- [19] **Yang, K. J., He, H. B., Ke, G. and Li, G. Y.** Application and test of miniature gas bearing turbines Advances in Cryogenic Engineering (1990), V35, 997-1003
- [20] **Sixsmith, H. and Swift, W.** A pair of miniature helium expansion turbines Advances in Cryogenic Engineering (1982), V27, 649-655
- [21] **Kato, T., Kamiyauchi, Y., Tada, E., Hiyama, T., Kawano, K., Sugimoto, M., Kawageo, E., Ishida, H., Yoshida, J., Tsuji, H., Sato, S., Xakayama, Y., Kawashima, I.,** Development of a large helium turbo-expander with variable capacity Advances in Cryogenic Engineering (1992), V37B, 827
- [22] **Kato, T., Yamaura, H., Kawano, K., Hiyama, T., Tada, E., Xakayama, Y., Kawashima, I., Sato, M., Yoshida, J., Ito, N., Sato, S. and Shimamoto, S. A.** Large scale turboexpander development and its performance test result Advances in Cryogenic Engineering (1990), V35, 1005–1012

- [34] **L'Air Liquide, France** www.airliquide.com
- [35] **Marot, G. and Villard, J. C.** Recent developments of air liquide cryogenic expanders
Advances in Cryogenic Engineering (2000), V45, 1493-1500
- [36] **Jadeja, H. T., Mitter, A. and Chakrabarty, H. D.** Turboexpander application for
cryoprocessing of nitrogen and related gases Proceedings of INCONCRYO85 Indian
Cryogenic Council Tata McGraw (1985), 85-101
- [37] **Mitter, A., Jadeja, H. T. and Chakrabarty, H. D.** Mechanical reliability and
manufacturing process for indigenous development of turboexpander Proceedings of
INCONCRYO-88 Indian Cryogenic Council (1988), 331-337 161
- [38] **Ghosh, P.** Analytical and Experimental Studies on Cryogenic Turboexpanders Ph.D
dissertation, IIT Kharagpur
- [39] **Akhtar M. S.** Selection and Optimisation of Centrifugal Compressors for oil and gas
applications. Using computers in the design and selection of fluid machinery I.Mech.E
(1993), 29-41
- [40] **von der Nuell, W. T.** Single - stage radial turbine for gaseous substances with high
rotative and low specific speed Trans ASME (1952), V74, 499-515
- [41] **Balje, O. E.** A contribution to the problem of designing radial turbomachines Trans
ASME (1952), V74, 451-472
- [42] **Balje, O. E.** A study on design criteria and matching of turbomachines: Part-A—
similarity relations and design criteria of turbines Trans ASME J Eng Power (1972), 83-
101
- [43] **Cartwright, W. G.** Specific speed as a measure of design point efficiency and optimum
geometry for a class of compressible flow turbomachines Scaling for performance
prediction in rotordynamic machines I Mech E (1978), 139-145
- [44] **Balje, O. E.** A study on design criteria and matching of turbomachines: part-b--
compressor and pump performance and matching of turbocomponents Trans ASME J
Eng Power (1972), 103-114

- [45] **RohliK, Harold E.** Analytical determination of radial inflow turbine geometry for maximum efficiency NASA TN D-4384 (1968)
- [46] **Luybli, R. E. and Filippi, R. E.** Performance options for cryogenic turboexpander AIChE symposium on Cryogenic properties, processes and applications (1986) V82, 24-33
- [47] **Vavra, M. H.** The applicability of similarity parameters to the compressible flow in radial turbomachines Proc Ins Mech Eng Internal Thermodynamics (Turbomachine 1970), 118- 132
- [48] **Whitfield, A.** Non-dimensional conceptual design of radial inflow turbines Radial Turbines Part B: Application of empirical correlations
- [49] **Denton, J. D.** The turboexpander - a design, make and test student project ASME-96-GT-191 (1996)
- [50] **Wallace, F. J.** Theoretical assessment of the performance characteristics of inward radial flow turbines Trans ASME (1958), 931-952
- [51] **Hasselgruber, H.** Stromungsgerechte gestaltung der laufrader von radialkompressoren mit axialem laufradeintrict Konstruktion (1958), 10(1) 22(in German)
- [52] **Ghosh, S.k.** “Experimental and Computational Studies on Cryogenic Turboexpander” Ph.D dissertation, NIT Rourkela.
- [53] **Ghosh, S.K., Sahoo, R.K., Sarangi, S.K.** “Computational Geometry for the Blades and Internal Flow Channels of Cryogenic Turbine.”
- [54] **Ghosh, S.K., Sessaiah, N., Sahoo, R.K., Sarangi, S.K.** Design of Turboexpander for Cryogenic applications, Indian Journal of Cryogenics, Special Issue - Vol.2, 75-81, (2005).